Proc Indian Natn Sci Acad **81** No. 2 March 2015 pp. 357-379
© *Printed in India*. DOI: 10.16943/ptinsa/2015/v81i2/48093

Review Article

Recent Progress in the Realm of Homonuclear Ln_6 Single Molecule Magnets: Structural Overview and Synthetic Approaches

SOUMYA MUKHERJEE and SUJIT K. GHOSH*
Indian Institute of Science Education and Research (IISER) Pune, Dr. Homi Bhabha Road, Pashan, Pune 411 008, India

(Received on 24 April 2014; Revised on 22 October 2014; Accepted on 30 October 2014)

The synthetic approaches to design hexanuclear Lanthanide-based single molecule magnets are demonstrated in detail. Extensive analysis of the reported hexanuclear systems provides vital insight for controlling the relaxation dynamics of Ln(III)-based SMMS. The assembly of hexanuclear lanthanide-based SMMs employing several ligands is summarized. Favorable structural units could be exploited as motifs in the formation of novel Ln(III)-based SMMs, slow magnetic relaxation feature being the principal focus for them. This review will span a number of hexanuclear homometallic 4f-complexes, which have been critical in the understanding of the manner in which the lanthanide centers in a complex interact magnetically. Heterometallic 3d-4f complexes which also present hexanuclearity are purposefully evaded to merely streamline and simplify the discussion in a much focused manner. Hexanuclear lanthanide model has particularly been the recent focus of attention to study and comprehend the magnetic coupling in 4f systems. This is to draw imperative conclusions concerning the most effective super-exchange pathways permitting the most efficient intracomplex interactions by demonstrating the research developed in the last few years on the fascinating field of Ln_6-based SMMs with precise emphasis on how recent studies tend to address the issue of relaxation dynamics in these systems from synthetic point of view.

Key Words: Lanthanide; Single Molecule Magnet; Synthetic Strategies; Slow Magnetic Relaxation; Anisotropy

Introduction

The promise of a realistic insurgence in the field of information technology, triggered by the rapid development in high-speed computers and high-density information storage devices has been driven by the keen interest over nanoscale magnetic materials for the last two decades, since the discovery of the first single molecule magnet in the early 1990s (Caneschi *et al.,* 1991; Sessoli *et al.*, 1993; Sessoli *et al.,* 1993; Gatteschi *et al.,* 1994). Huge enthusiasm followed the stupendous discovery of this dodecametallic manganese-acetate cage $[Mn_{12}O_{12}(OAc)_{16}(H_2O)_4]$, which for the first time showed the unique property of retaining the magnetization for long time periods in the absence of any external magnetic field. This famous transition metal coordination compound established itself as the progenitor of an enormous family of magnetic materials, known as single molecule magnets (SMMs) (Zaleski *et al.,* 2004; Gatteschi *et al.,* 2006; Lin *et al.,* 2008; Costes *et al.,* 2008; Chibotaru *et al.,* 2008; Gamer *et al.,* 2008; Zheng *et al.,* 2009; Burrow *et al.,* 2009; Xu *et al.,* 2010; Ishikawa *et al.,* 2003; Luzon *et al.,* 2008; Lin *et al.,* 2009; AlDamen *et al.,* 2008; Cardona-Serra *et al.,* 2012; Joarder *et al.,* 2012), which could be precisely defined as such

*Author for Correspondence: E-mail: sghosh@iiserpune.ac.in; Tel: +91 20 2590 8076

molecular species, essentially aggregates possessing both non-negligible high-spin ground state (*S*) and uniaxial (negative) Ising-like magnetic anisotropy |*D*| (taking into account the Hamiltonian: $H = DS_z^2$), leading to an anisotropy energy barrier (U) ($S^2|D|$ or $(S^2\text{-}1/4)|D|$ for integer or half integer spins respectively, for the reversal of magnetization (Habib *et al.,* 2013; Chakov *et al.,* 2006). One remarkable aspect is that, this relationship applies satisfactory to 3d and 4d-transition metal systems but is unable to represent correctly the experimental barriers in lanthanide complexes. For lanthanide-based SMMs comprising of 4f-orbitals, more anisotropic terms are required (in addition to *D*), for an accurate illustration of *U* (Chibotaru *et al.,* 2008; Habib *et al.,* 2013). Herein, each molecule acts as a single domain magnetic nanoparticle. Lanthanide SMMs have been an important research focus due to large relaxation barriers along with hysteresis loop openings clearly surpassing any other metal systems. The single-ion anisotropy of lanthanide ions is enormously large compared to the 3d- and 4d-metal analogues. That is the basic reason for which the last decade has observed a remarkable progress in the magnetism-oriented studies for these intriguing lanthanide complexes (Ishikawa *et al.,* 2008; Milios *et al.,* 2007; Yoshihara *et al.,* 2008; Magnani *et al.,* 2010; Guo *et al.,* 2010; Jiang *et al.,* 2011; Watanabe *et al.,* 2011; Gonidec *et al.,* 2010; Rinehart and Long 2011).

Notwithstanding the enormous inherent interest in SMMs, it was also understood that they could, in principle be developed for new technological applications following a strategy-based rational approach (Hussain *et al.,* 2009; Hewitt *et al.,* 2009; Long *et al.,* 2011; Chen *et al.,* 2011; Guo *et al.,* 2011; Lin *et al.,* 2012; Xue *et al.,* 2012; Tian *et al.,* 2012; Anwar *et al.,* 2012; Habib *et al.,* 2012). Entirely novel applications of SMMs have recently been envisaged, including the advancement in the field of molecular spintronics (Leuenberger *et al.,* 2001; Coronado *et al.,* 2004; Ardavan *et al.,* 2007; Bouchiat *et al.,* 2008; Bogani *et al.,* 2008; Mannini *et al.,* 2010; Urdampilleta *et al.,* 2011; Rinehart *et al.,* 2011; Katoh *et al.,* 2012). However, SMM-based technology can only be practically achieved when two major problems gets solved. Firstly, the distinctive properties of SMMs are presently accessible only by means of liquid helium cooling; consequently, either the operating temperatures need to rise considerably, or applications arising out of these materials prove so significant, that temperature ceases to be a relevant issue. Secondly, addressing individual molecules of SMMs on surfaces have only been explored with rare examples (Woodruff *et al.,* 2013). Therefore, one of the imposing challenges in this field is to design and synthesize efficient SMMs which function at ambient temperatures prospective of practical use, or which exhibit properties that goes beyond the limits achievable by the domain of classical magnets.

Underlying Physics and Subsequent Characterization Protocol

A current review by Rinehart and Long (Rinehart and Long 2011) offers a coherent account of how f-element electronic structures can, in principle, be exploited to build up novel SMMs. In this segment, we sum up the main features of lanthanide (Ln) electronic structures that are imperative to deduce the characteristics of Ln-SMMs. Irrespective of the metal-type, the two precise prerequisites for a molecule to behave as an SMM are that the electronic ground state have got to be bistable, and that magnetic anisotropy should be present as an essential attribute. For Ln ions possessing ground electronic terms other than $^1S_0$ and $^8S_{7/2}$, the orbital contribution to the magnetic moment is quite large and unquenched, while the ligand field effects in lanthanide complexes can be considered as small-yet-significant perturbation (Wybourne 1965; Abragam and Bleaney 2012). On the contrary, for transition metals (TM) belonging to 3d-series, spin-orbit coupling is secondary to ligand field effects; consequently Ln-SMMs differ from transition metal SMMs primarily in the nature of their bistable ground state. For TM-SMMs, the total spin S and the resulting $[2S + 1]$ m_S substates lead to ground-state bistability (Gatteschi *et al.,* 2006). In comparison, for Ln-SMMs, ground-state bistability develops from the $[2J + 1]$ m_J microstates within the spin-orbit-coupled ground term, $(2S+1)$ L_J. Merely taking into account the number of unpaired electrons offers only a small insight into the magnetic properties of lanthanide

ions. An auxiliary characteristic (not a stern prerequisite) of the metal ions in Ln-SMMs is that the ground state must have a high value of m_J, which transcends into a substantial magnetic moment value. Henceforth, the lanthanide ions most frequently used in SMMs are Tb(III), Dy(III), Er(III), and Ho(III). Due to the strong angular dependence of the 4f orbitals, the Tb(III) and Dy(III) ions' electronic structures possess significant anisotropy: the vast majority of Ln-SMMs include either terbium or dysprosium, and in Ln-SMMs comprising of two or more lanthanide ions, Dy(III) is omnipresent. It is also worth mentioning that even though Dy-SMMs simply outnumber Tb-SMMs, the latter group comes up with some of the largest U_{eff} values. In a simple estimation, this order can be interpreted in terms of electronic structure. Dy-SMMs have quite large U_{eff} values because Dy(III) ions have high magnetic anisotropy, and the energy gap between ground and first excited m_J levels is mostly considerably high. Dy(III)-SMMs are the most populated ones among the class of SMM materials, because dysprosium(III) is a Kramers' ion (it has an odd number of f-electrons), clearly referring to a bistable ground state, albeit the ligand field symmetry. Some Tb-SMMs have very large U_{eff} values because Tb(III) can have greater magnetic anisotropy and larger Δm_J gaps than Dy(III); however, there are fewer Tb-SMMs because terbium(III) is a non-Kramers' ion, meaning that the ground state is only bistable when the ligand field has axial symmetry. The protocol primarily adhered to aimed at the design of SMMs is the strategic employment of the ligand field symmetry to enhance the single-ion anisotropy of Ln^{3+} (Rinehart and Long, 2011). Ligands those are able to generate an axially symmetrical complex should enhance the anisotropy, simply based on an electrostatic model, and for Ln-SMMs containing one solitary lanthanide ion; this basis has in fact been remarkably successful. More the number of Ln(III) ions in the SMM, the control over the symmetry of the coordination environments turns out to be increasingly unfeasible, and our assessment of the literature has found out the general trend of diminishing SMM properties with expansion in molecular structures.

SMMs are conventionally characterized in crystalline forms by means of magnetic property measured by magnetometers, mainly SQUID. The standard test adopted to ascertain the credentials of an SMM includes measurement of the magnetic susceptibility (χ) by the use of a small amount of alternating current (ac), or dynamic magnetic field of about 1-5 Oe, over a range of temperatures (T = 1.5-50 K accounts for the majority of SMMs). Using a typical magnetometer, the frequency ν of the ac field can generally be changed in the range of 1-1500 Hz and as a result, the ensuing time-dependent magnetic moment can be appropriately characterized by a finite relaxation time, τ, at a specified temperature. Since each of the SMM molecules have their individual magnetic moment, the total magnetization of a bulk SMM sample will lag behind the driving ac field as it alternates, across the sample, in such a way that the actually measured magnetic susceptibility will draw in a phase shift into the same. This experiment leads to the in-phase and out-of-phase susceptibilities, denoted respectively by χ' and χ''. One of the most reliable methods of recognizing and characterizing an SMM is to inspect the variation of χ' and χ'' with temperature at quite a few different frequencies. As the temperature decreases, if the plot of χ'' steadily increases to reach a maximum and later followed by a decline, then this is indicative of the blocking of spin reversal phenomenon. Moreover, with changing ac frequency, the position of the maximum in the $\chi''(T)$ plot also undergoes a dependent alteration. Likewise, plots of $\chi''(\nu)$ at varying temperatures are also extensively exploited to confirm SMM behavior. The lack of maxima in the $\chi''(T)$ plots, or the absence of frequency-dependent χ'' in zero field leads to indistinctness over precise SMM characteristics. The $\chi''(\nu)$ isotherms also afford the most unfailing means of determining the energy barrier to magnetization reversal, or the anisotropy barrier, U_{eff}. Each $\chi''(\nu)$ curve permits to ascertain an average relaxation time, τ, at a given temperature (Morrish, 1966), and the relationship of τ with temperature is given by the well-known equation:

$$\tau = \tau_0 \exp(U_{eff} / k_B T) \quad (1)$$

Equation 1 is an Arrhenius-type correlation, and so it can be employed to find out the anisotropy barrier from the slope of the plot of $\ln\tau$ versus T^{-1}, where the graph is linear and $\ln\tau$ is dependent on temperature. When these set of criteria are achieved, the SMM magnetization is said to relax via a thermally assisted mechanism. The physics can be nicely demonstrated and explained by an Orbach process, in which there are two energetically low-lying degenerate states of the lanthanide ion, and an excited state that lies above the ground state by U_{eff}. When the lanthanide ion in the low-lying state with $m_J = +J$ absorbs a phonon with a frequency equivalent to U_{eff}, it can attain the excited state and then relax to the other low-lying state with $m_J = -J$. This temperature-dependent process imparts a thermal equilibrium between the two components of the degenerate ground state, ensuing in relaxation of the magnetization (Abragam and Bleaney, 2012). The other two substitute relaxation mechanisms are the direct process and the Raman process, in which phonons can result into a "spin flip" within the ground doublet. For a high number of Ln-SMMs, the Arrhenius plots are marked with linearity, possessing a positive gradient across a restricted temperature range, and quite often at lower temperatures the plot will come up with a series of consecutive data points for which $\ln\tau$ is independent of the temperature. By means of employing Tb (III) as the example again, occurrences when the Arrhenius plot's gradient turns out zero provide apposite evidence in support of the magnetization relaxing from $m_J = +6$ to $m_J = -6$, by quantum tunneling of the magnetization (QTM) (Woodruff *et al.,* 2013). Arrhenius plot-regions falling between the two limits of extremes generate signature curvature profiles in $\ln\tau$ versus T^{-1}, implying the concurrent nature of the thermal and the QTM mechanisms. The qualitative depiction as described above belies the intricate nature of the relaxation process of the magnetization in Lanthanide-SMMs. As the following sections describe, it is pretty usual for more than one thermally activated mechanism to take place in a SMM, and it is simultaneously possible for the magnetization to get relaxed more or less exclusively via QTM. To find out the occurrence of several relaxation processes is comparatively uncomplicated to perform by modeling ac susceptibility data (including the Cole-Cole plot of χ' vs χ''). To gain an ample understanding on why such phenomena happen in the way that they do is much more exigent. This is undoubtedly one of the most motivating aspects in the field: diverse procedures for synthesizing and characterizing Ln-SMMs are although quite well-developed; nevertheless, theoretical understanding of their fascinating properties is still on a evolving stage.

Hexanuclear Lanthanide SMMs

The fundamental questions regarding single-ion relaxation versus slow relaxation arising from the molecule as an individual entity can be solved employing hexanuclear lanthanide SMMs, since they are undoubtedly one of the extremely important model systems. Systematic and strategic variations in the used ligand spacers were implemented in order to achieve a correlation of the ligand's influence on the molecular architecture as well as over the orientation of anisotropic axes on lanthanide centers (Lin *et al.*, 2009; Murugesu, 2012). The key component of these SMM systems, which binds the constituent metal ions in adjacent proximity, involves the usage of ligands with oxygen-donor functionalities capable of acting as bridges between the metal ions (Anwar *et al.,* 2012; Palacios *et al.,* 2014; Zhang *et al.,* 2013). *o*-Vanillin and phenolic based ligands have given rise to triangle-based Dy(III) complexes demonstrating SMM behaviour, with examples comprising of trinuclear, tetranuclear and hexanuclear cluster cores (Zhang *et al.,* 2013; Costes *et al.,* 2001). Typically the three Dy(III) ions are bridged by μ_3-O connections within each metallic triangle, and also encompass μ_2-O bridges within the triangles and between such triangles. In the reported Dy_4 and Dy_6 cases, the basic μ_3-O bridged triangular entities are frequently interconnected to form 'butterfly' and edge or end shared geometries respectively (Randell *et al.,* 2013). Slow magnetic relaxation and SMM behavior are practically observed in almost all of the cases, with combinations of interlinked triangles.

In fact, there are two distinct categories of

hexanuclear cluster systems displaying SMM behaviour, based on the arrangement of the metal centers in their cores. Typically, the first category is represented by symmetric arrangement of the six metal centers to construct a metallic wheel/ring, while the other category is typified by the relatively more familiar combinations of interconnected triangles. Rather than distinguishing these SMM materials based on the symmetry-aspect, it seems more judicious to divide the entire regime of the reported hexanuclear SMMs into two more general broad classifications: First class being the homonuclear Ln_6 series where the metal centers are solely 4f-elements, whereas the second class comprises of the heteronuclear entities composed of both 3d- and 4f-metal centers (Randell *et al.*, 2013; Boskovic *et al.*, 2002; Brechin *et al.*, 2002; King *et al.*, 2004; Zheng *et al.*, 2007; Manoli *et al.*, 2007; Feng *et al.*, 2010; Stamatatos *et al.*, 2011; Nayak *et al.*, 2010; Kotzabasaki *et al.*, 2011; Yang *et al.*, 2011; Costa *et al.*, 2012; Charalambous *et al.*, 2012; Chakraborty *et al.*, 2012; Mukherjee *et al.*, 2014). Hereafter, our discussion will revolve around the first class only. In this particular class, encompassing all the literature reports in the homonuclear Ln_6 regime, it was observed that barely a single report of Ln_6 homometallic wheel came up through all these years, as compared to the eight structures typified by the combinations of interconnected Ln_3 triangles.

Homonuclear Ln_6 SMMs

Murugesu *et al.*, as early as 2009, reported the first such example of a unique Dy^{III}_6 complex formed by the coupling of two similar Dy^{III}_3 triangles, in which intramolecular ferromagnetic interactions and single-molecule magnetic behaviour was witnessed (Hussain *et al.*, 2009). In an effort to create new-generation smarter lanthanide SMMs with large anisotropic barriers and also to grasp the inimitable properties of such systems, Ln_3 complexes were employed as building blocks to create larger SMMs by using the simple synthetic approach (Milios *et al.*, 2006). whereby reaction of a Ln^{III} metal centre, $Dy(NO_3)_3$, and *o*-vanillin occurs in the presence of a strong base (KOH) and acetone as solvent. These modified reaction conditions lead to an *in situ* aldol condensation reaction between some of the *o*-vanillin molecules and acetone, forming a newfangled aldol ligand (Palomo *et al.*, 2002) that assists to unite two Dy^{III}_3 triangular motifs in a mixed-ligand complex. Therefore report synthesis, structure and magnetic properties of a rare ferromagnetically coupled Dy^{III}_6 SMM obtained using a synthetic block building approach. The complex **1**, having formula $[Dy^{III}_6(\mu_3\text{-}OH)_4(ovn)_4(avn)_2(NO_3)_4(H_2O)_4](NO_3)_2(H_2O)_3(CH_3)_2CO$, interestingly contained two different types of ligands, *o*-vanillin (ovnH) and aldol-vanillin ($avnH_2$), among which the latter was a *in situ* aldol condensation reaction product from *o*-vanillin and the reaction solvent, acetone (Fig. 1). The dc magnetic susceptibility of **1** was measured in an applied magnetic field of 1000 Oe and can be seen plotted as χT vs. T (in which χ is the molar magnetic susceptibility) in Fig. 2B. The χT value at 300 K of 86.6 $cm^3K\ mol^{-1}$ is close to the expected value of

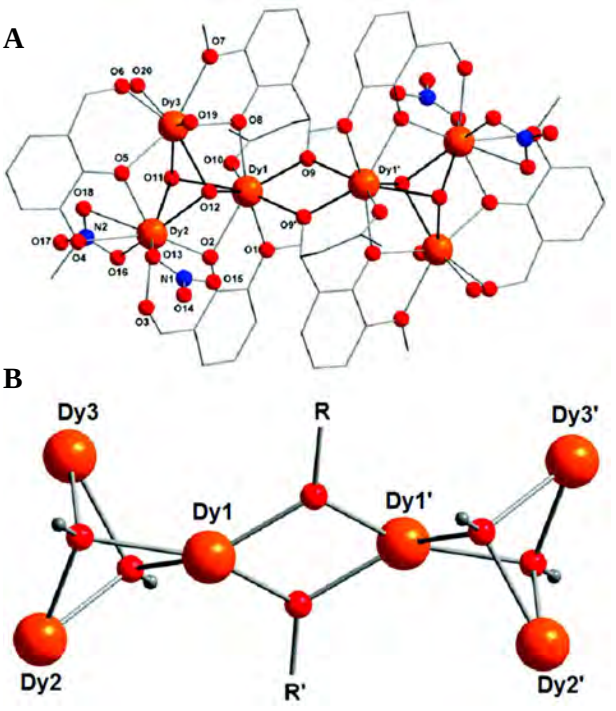

Fig. 1: (A): The molecular structure of 1, showing one of the two isomers. Solvents, counter ions and hydrogen atoms are omitted for clarity. Symmetry equivalent positions are denoted by a prime in the label. Colour code: orange (Dy), red (O), blue (N), grey (C); (B): The $[Dy_6(\mu_3\text{-}OH)_4(OR)_2]$ core (R= avn^{2-}). Colour code: orange (Dy), red (O), grey (H). (Hussain *et al.*, 2009)

85.02 $cm^3K\ mol^{-1}$ if the six Dy^{III} ions ($S = 5/2$, $L = 5$, $^6H_{15/2}$, $g = 4/3$) were non-interacting, and it gradually increases with decreasing temperature to reach a maximum of 105.8 $cm^3K\ mol^{-1}$at ~42 K, before decreasing to 26.7 $cm^3K\ mol^{-1}$ at 1.8 K. The increase of the χT product suggests the presence of a dominant intramolecular ferromagnetic interaction between the Dy^{III} ions. The low temperature decrease is likely due to a combination of intermolecular antiferromagnetic interactions, large magnetic anisotropy and thermal population of the excited states of the Dy^{III} ions. The non-superposition of the *M* vs. *H/T* data (Fig. 2B, inset) on a single master curve and the high-field non-saturation suggests the presence of significant magnetic anisotropy and/or low lying excited states in complex **1**. The temperature-dependent ac susceptibility of **1** was measured under zero-dc field (Fig. 2B). At low temperatures below ~18 K, an out-of-phase (χ'') ac signal indicating a slow relaxation of magnetization is observed. The shape and the frequency dependence of the ac susceptibility signal indicate the SMM nature of **1**. Henceforth, single-crystal dc relaxation measurements were performed on a micro-SQUID in the temperature range 1.1-0.04 K to further inspect the low temperature behavior (Fig. 2C). Below 1 K, unusual two-step shaped hysteresis loops were observed with an opening of the loops at a temperature of ~1 K. The coercivity of the loops increases continuously for lower temperatures and reaches a maximum around 0.2 K.

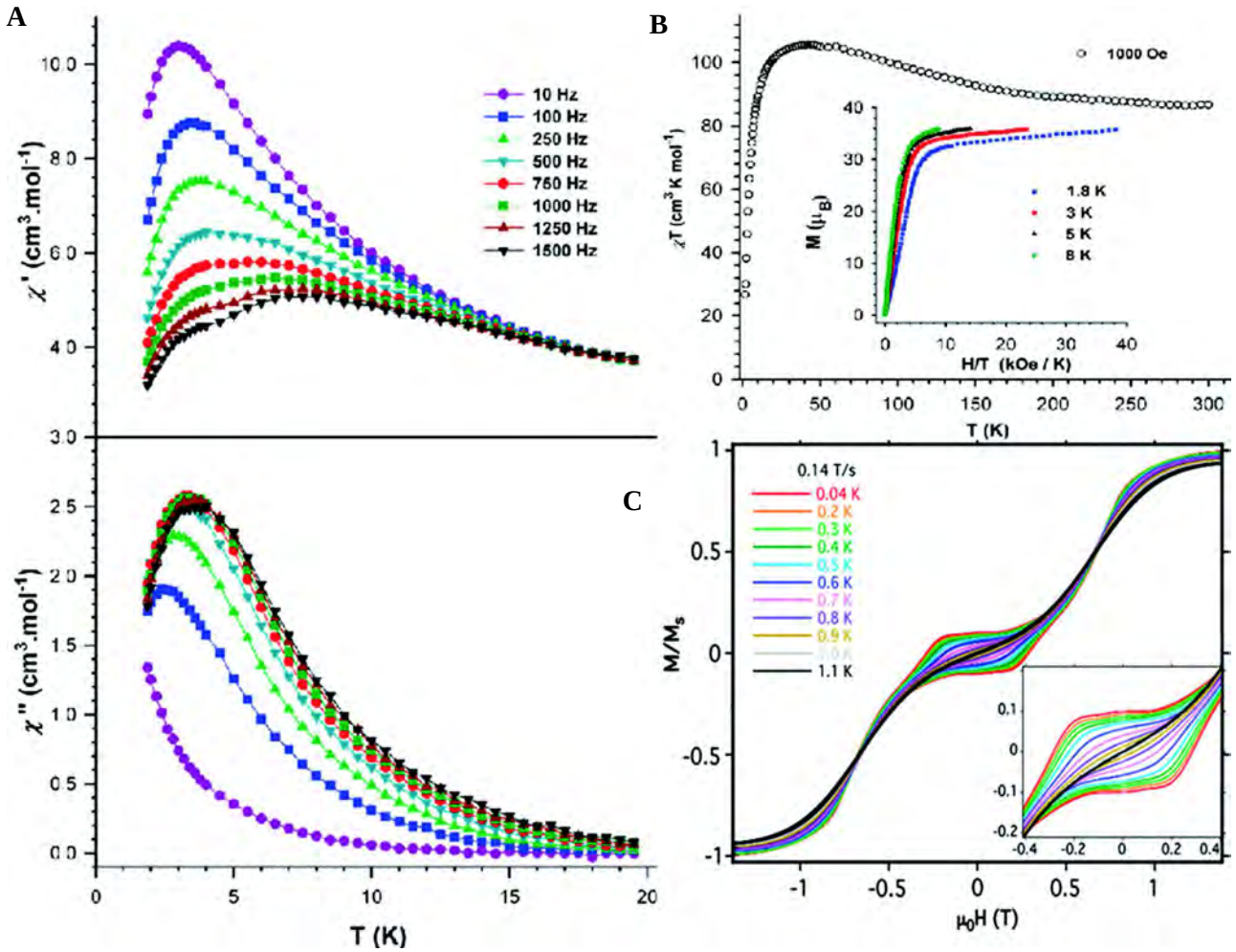

Fig. 2: (A): Temperature dependence of the in-phase (top) and out-of phase (bottom) ac susceptibility of 1 under zero-dc field; (B): Plot of $\chi_m T$ vs. *T* for complex 1 at 1000 Oe. Inset: *M* vs. *H* data at various temperatures are shown on a single *M* vs. *H/T* plot; (C) Magnetization (*M*) vs. applied dc field sweeps at the indicated sweep rate and temperatures. *M* is normalized to its saturation value, M_s, at 1 T. Inset: zoomed in central portion of the hysteresis loops (Hussain *et al.*, 2009)

Below this temperature the loops become temperature independent. This behaviour further confirms the SMM nature of **1** with very slow zero-field relaxation.

By carefully tuning the reaction conditions, this first report of Dy_6 SMM was actually an innovative attempt to dimerize the highly anisotropic Dy_3 building blocks by the mediation of *in situ* generation of a novel aldol ligand. The Dy_6 complex exhibited slow relaxation of magnetization accompanied by frequency-dependent out-of-phase signal and hysteresis loops below 1.1 K with temperature independence below 0.2 K. Such distinctive behaviour evidently established SMM features for complex **1**. This hexanuclear lanthanide SMM demonstrating intramolecular ferromagnetic interactions between Dy^{III} ions still presents one of the toughest synthetic challenges in lanthanide SMM chemistry to strategically couple two anisotropic units aimed at maximization of toroidal magnetic moment, with high blocking temperatures (T_B).

Following the similar trend of coupling toroidal Dy_3 triangles to generate a Dy_6 SMM, Sessoli and Powell *et al.* came up with one more fascinating example in the ensuing year (Hewitt *et al.*, 2010). This time, the SMM on focus, $[Dy_6(\mu_3\text{-}OH)_4L_4L'_2(H_2O)_9Cl]Cl_5\cdot 15H_2O$ (compound **2**), was a result of adopting mixed ligand strategy, the participating ligands being *o*-vanillin (HL) and 2-hydroxymethyl-6-methoxyphenol being H_2L' respectively (Fig. 3B). The Dy_6 structure in this present complex can be perceived as one ensuing from the formal linkage between the alkoxides of the reduced form of both the ligands of two of the constituent triangular Dy_3 units (Tang *et al.*, 2006), accompanied by the simultaneous loss of two of the terminal chloride ligands.

Using AC susceptibility measurements, the magnetization dynamics were thoroughly investigated, with remarkable outcomes in zero static fields presented in Fig. 3. Circumventing the detailed analysis of the obtained magnetic data, the formal linking of two Dy_3 units to constitute the hexanuclear Dy_6 entity gave rise to a spectacular escalation in the temperature at which slowing down of the magnetization was observed from 8 to 25 K. An unprecedented transformation in the nature of the magnetic anisotropy from an easy plane to easy axis type on increasing the temperature is mainly attributable behind the observation of two distinct relaxation regimes. This variation was clarified by breaking the symmetry brought about by connecting the two triangles. This observed behavior was exactly opposite to the commonly encountered scenarios for anisotropic systems with decreasing temperature,

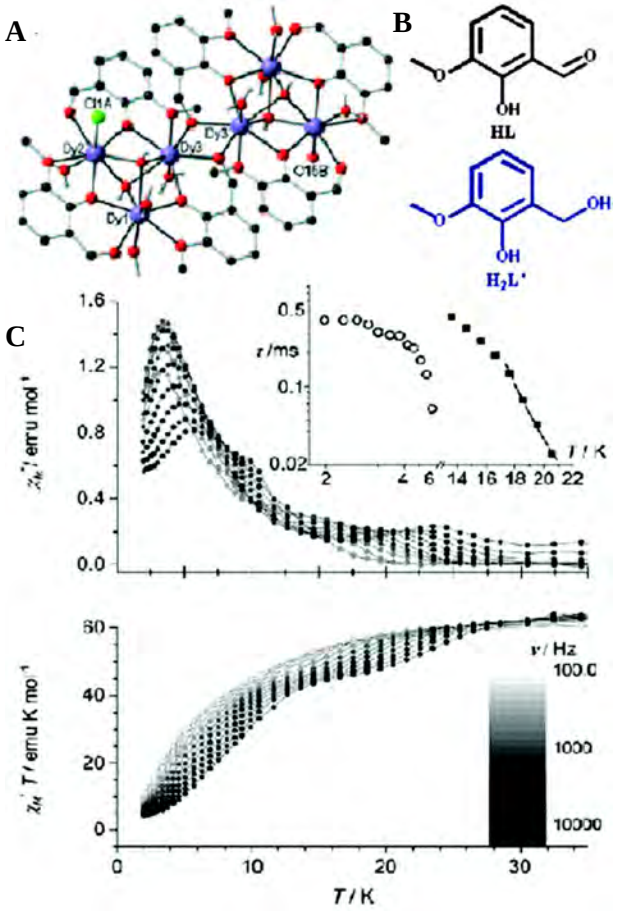

Fig. 3: (A): Structure of the $[Dy_6(\mu_3\text{-}OH)_4L_4L'_2Cl(H_2O)_9]^{5+}$ cation in complex 2 (Dy: blue, Cl: green, O: red); (B): Structural formulae for the employed ligands: *o*-vanillin, HL, (top) and 2-hydroxymethyl-6-methoxyphenol, H_2L' (bottom); (C): Top: Field dependence of the molar magnetization measured on a pellet of polycrystalline powder of Dy_6 at T=1.8 K (●) and T=4.0 K (□). Bottom: Temperature dependence of AC magnetic susceptibility for Dy_6 of imaginary component and $\chi'T$ product in zero static field. Inset: temperature dependence of the relaxation time for the low temperature (■) and high-temperature (○) processes are shown; the high-temperature data is fitted using the Arrhenius law (—). Reprinted with permission from Ref. Hewitt *et al.*, 2010. Copyright (2010) Wiley-VCH

where they are expected to become more, rather than less anisotropic at low temperature. It was indeed an exciting discovery at the mentioned juncture of Ln-SMM research, as a relatively long relaxation time, worthwhile for molecular spintronics device-applications, could be achieved at high temperatures owing to the excited state-properties.

Employing the well-known ligand triethanolamine ($teaH_3$), Murray *et al.* reported colourless crystalline complexes $[Ln_6(teaH)_6(NO_3)_6]\cdot 8MeOH$ (Ln = Dy (**3**), Gd (**4**)) in the same year, which exhibited slow relaxation of magnetization (Langley *et al.*, 2010). These could be isolated merely by reacting $Ln(NO_3)_3\cdot 6H_2O$ (1 mol. equiv) with $teaH_3$ (1 mol. equiv), and triethylamine in methanolic medium. Complexes **3** (shown in Fig. 4A) and **4** crystallize in the trigonal space group *R-3* and form Dy^{III} and Gd^{III} 6-wheel clusters. Each of their asymmetric unit contains one unique Ln(III) ion with one $teaH^{2-}$ and one NO_3^-, with one methanol solvent molecule at full occupancy with another lying on the crystallographic *c*-axis at one-third occupancy. Interestingly, these were the first hexanuclear 4f wheel compounds till now, which has proved to be the solitary report in the homonuclear Ln_6 domain under discussion. There is noteworthy intermolecular hydrogen bonding within complexes **3** and **4**, each

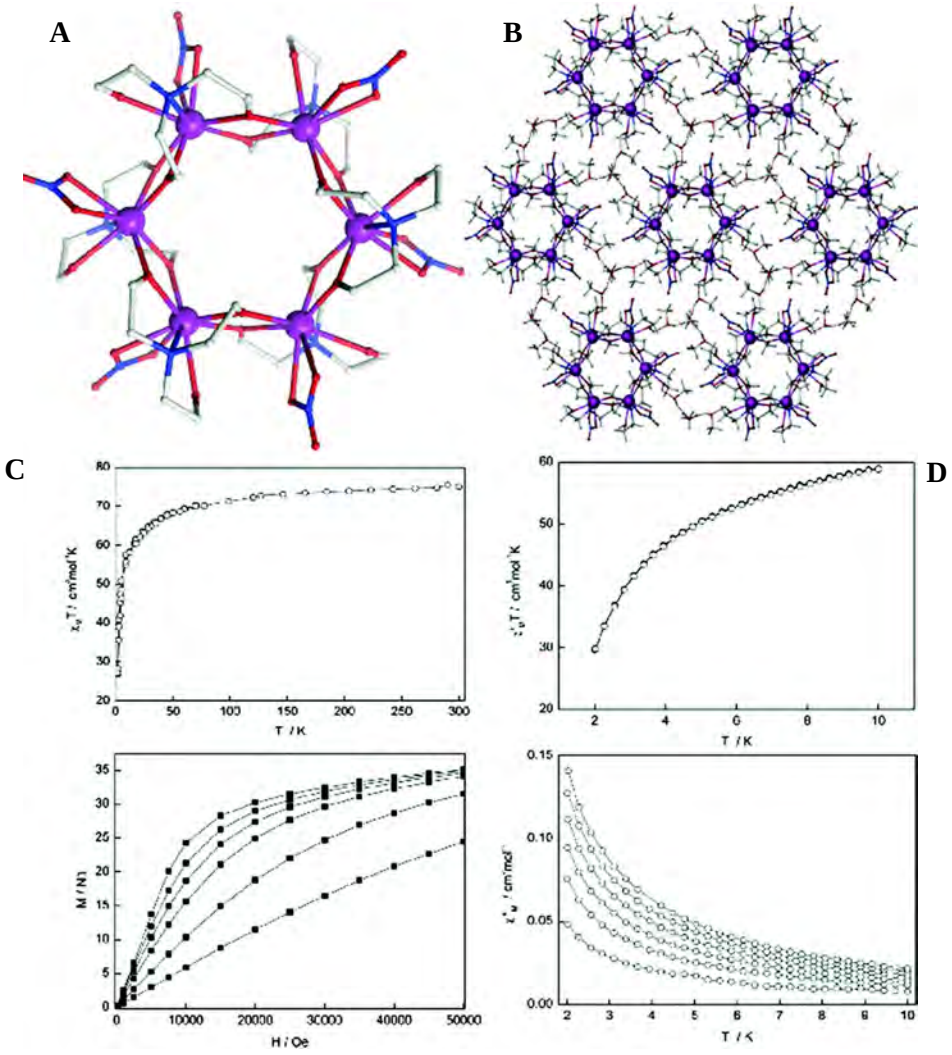

Fig. 4. (A): Weblab viewer representation of compound 3; (B): Hydrogen-bonded packing arrangement in 3; (C): top: plot of $\chi_m T$ vs. T for 3, in fields of 1 T and 0.1 T (70-2 K), bottom: plots of isothermal magnetization, *M* (in $N\beta$), vs. field (0-5 T) at temperatures 2 (top), 3, 4, 5.5, 10, 20 K (bottom); (D): Top: plots of $\chi_m' T$ vs. *T* for 3. Bottom: plots of χ_m'' *versus T* for 3 in AC frequencies 1500 (top), 1250, 1000, 750, 500, 250 (bottom) Hz. (Langley *et al.*, 2010)

protonated $teaH^{2-}$ ligand hydrogen bonds to a solvent molecule of MeOH which, in turn, forms hydrogen bonds to another disordered MeOH that lies on the crystallographic *c*-axis. This associates the constituent clusters in a hexagonal fashion (Fig. 4B). Plots of $\chi_m T$ *vs* *T* are presented in Fig. 4C. The room temperature $\chi_m T$ value of 76.0 $cm^3mol^{-1}K$ for **3** is lower as compared to the expected value for six uncoupled Dy^{III} ions of 85.01 $cm^3mol^{-1}K$ (S = 5/2, L = 5, $^6H_{15/2}$, g = 4/3, *C* = 14.17 $cm^3mol^{-1}K$). There is a slow and gradual decrease in the $\chi_m T$ values between 300 and ~70 K. $\chi_m T$ value then decreases quite briskly to reach a value of 26.0 $cm^3mol^{-1}K$ at 2 K. The decrease observed in the $\chi_m T$ values, and the negative *q* value, suggest the existence of weak antiferromagnetic interactions and probably other effects such as magnetic anisotropy/ligand field and thermal depopulation of the Dy^{III} excited states (Stark sublevels of the $^6H_{15/2}$ state), the latter being insignificant because of the equal $\chi_m T$ values being observed in fields of 1 T and 0.1 T between 70 and 2 K. The *M vs*. *H* data (Fig. 4C (bottom)) is also suggestive of the effects from low lying excited states and/or anisotropy, as the curve does not saturate and the values of *M* in the 5 T field, 34.5 $N\beta$, are alike at temperatures 2, 3 and 4 K. Considering both the in-phase ($\chi_m' T$) and out-of-phase (χ_m'') AC susceptibilities, the changes in AC frequencies had little effect on the $\chi_m' T$ plots, but showed a pronounced effect, below~7 K, on the χ_m'' plots, albeit without reaching the characteristic maxima above 2 K (Fig. 4D). Drawing a conclusion from the magnetic dataset for these Ln^{III} systems, a non-zero spin ground state is clearly encountered seemingly originating out if the closely spaced M_J Stark sublevels. AC susceptibility measurements for the Dy-analogue **3** also provided evidence for slow relaxation of the magnetization reversal.

As a related finding, in the same year, Wang and Liao *et al.* reported five new hexanuclear oxo-hydroxo lanthanide clusters having a general formula $[Ln_6(\mu_6\text{–}O)(\mu_3\text{–}OH)_8]^{8+}$ [Ln = Er(**5**), Ho(**6**), Dy(**7**), Gd(**8**), Tb(**9**)] employing 4-amido-3,5-dimethyl-1,2,4-triazole as ligand (Tong *et al.*, 2010). Notably, the oxo group plays the crucial role of an anion template to induce the self-assembly of lanthanide ions. The simplified view for this hexanuclear complex is presented in Fig. 5A, while the experimental variations of χ_M and μ_{eff} versus *T* for complex **8** is represented in Fig. 5B. As evident from Fig. 5B, upon cooling from 300 to 50 K, the μ_{eff} values gradually decrease; below 50 K, the μ_{eff} values rapidly decrease with further cooling, suggestive of a dominant antiferromagnetic interaction between the Gd^{3+} ions. Analogously, for complexes **5**, **6**, **7** and **9**, upon lowering temperature, μ_{eff} monotonically declines. This feature comes out principally because of the splitting of the ligand field of the Ln^{3+} ions due to strong spin-orbital coupling, and is partially

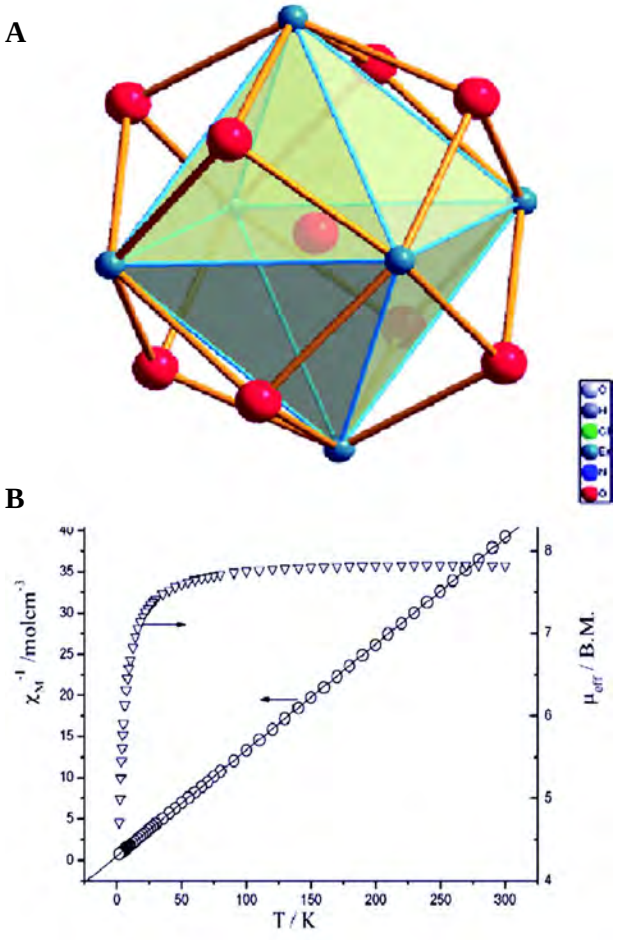

Fig. 5: (A): Simplified view of the hexanuclear $[Er_6(\mu_6\text{-}O)(\mu_3\text{-}OH)_8]^{8+}$ core structure emphasizing the lanthanide ions made as quasi-perfect octahedron (for simplicity, only oxygen atoms (red circles) and lanthanide ions (dark green circles) have been drawn; (B): Experimental variations of χ_M^{-1} (◆) and μ_{eff} (○) versus *T* for complex 4, the line represents the best fit to the Curie-Weiss law (Tong *et al.*, 2010)

contributed to the probable antiferromagnetic interaction between the Ln^{3+} ions.

The following year of 2011 beheld two highly significant reports published from the groups of Liu and Tang *et al*. A distinctive hexanuclear dysprosium(III) compound $[Dy_6(\mu_3\text{-}OH)_3(\mu_3\text{-}CO_3)(\mu\text{-}OMe)(HL)_6(MeOH)_4\text{-}(H_2O)_2]\cdot 3MeOH\cdot 2H_2O$ (**10**) was reported by Liu and Tang *et al.* (Tian *et al.*, 2011) constituted from a newfangled polydentate schiff-base ligand, which exhibited complex slow relaxation of the magnetization presumably concomitant with the single-ion behavior of individual Dy^{III} ions as well as the conceivable weak coupling between them. The reaction of $DyCl_3\cdot 6H_2O$ with the ligand in $MeOH/CH_2Cl_2$, in the presence of triethylamine, produces yellow crystals of the hexanuclear complex **10**. The structure comprises of two crystallographically unique, but structurally alike, Dy_6 units in the unit cell, each of them is illustrated in Fig. 6A. The hexanuclear core of complex **10** contains six Dy^{III} ions, which can be considered as the amalgamation of three capped triangular Dy_3 units.

The direct-current (dc) magnetic susceptibility studies for complex **10** were performed in a magnetic field of 1000 Oe in the temperature range 300-2 K. The plot of $\chi_m T$ vs T, where χ_m is the molar susceptibility, is displayed in Fig. 6B. The experimental $\chi_m T$ value at 300 K of 84.8 cm^3Kmol^{-1} corresponds unerringly to the anticipated value of 85.02 cm^3Kmol^{-1} for six uncoupled Dy^{III} ions (S = 5/2, L = 5, $^6H_{15/2}$, g = 4/3). $\chi_m T$ progressively declines until 50 K with an additional drop to reach a minimum of 68.6 cm^3Kmol^{-1} at 2 K, which is most likely attributed to the progressive depopulation of excited Stark sublevels, and the shoulder at low temperatures

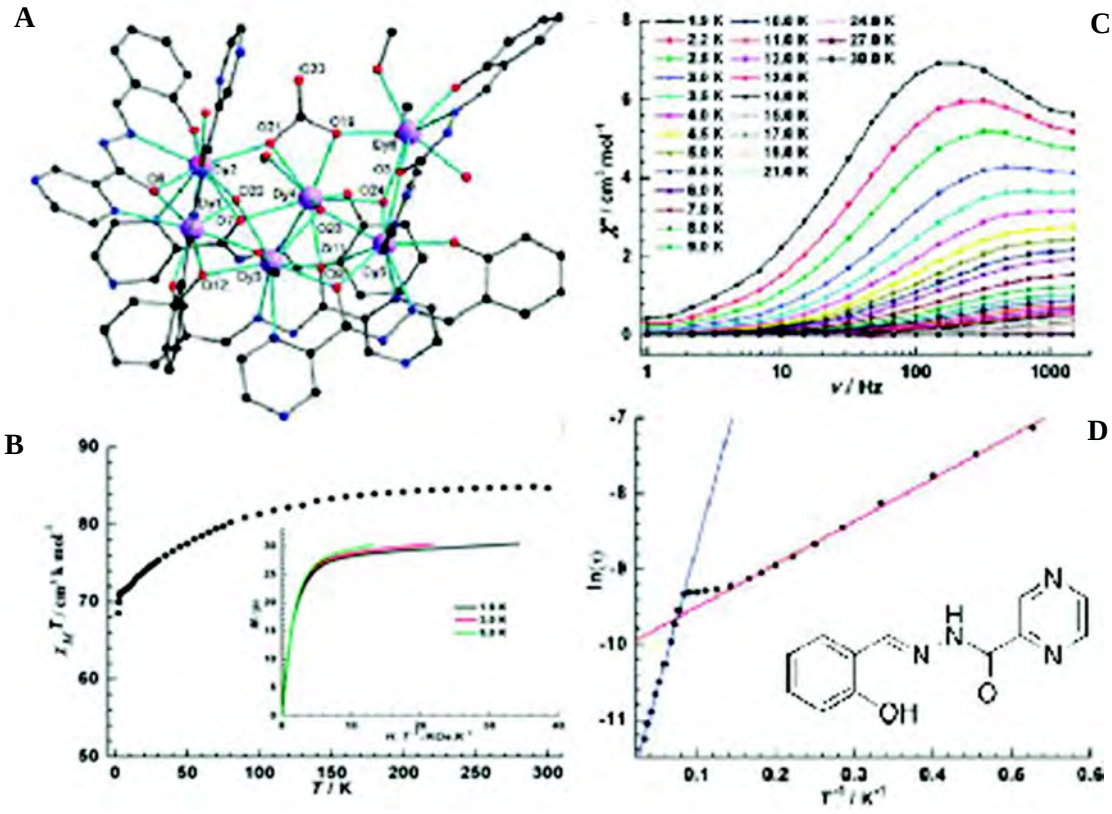

Fig. 6: (A): Molecular structure of complex 10. H atoms are omitted for clarity; (B): Temperature dependence of the $\chi_m T$ product at 1 kOe. Inset: *M vs H/T* plots at different temperatures below 5 K for complex 10; (C): Frequency-dependent out-of-phase ac susceptibility of 10 below 30.0 K under zero dc field; (D): Magnetization relaxation time, $ln\ \tau$, vs T^{-1} under zero dc field. The solid line is fitted with the Arrhenius law; (E): Structure of the ligand (E)-N´-(2-hydroxybenzylidene) pyrazine-2-carbohydrazide. [Reprinted with permission from Ref. Tian *et al*., 2011. Copyright (2011) American Chemical Society]

might propose a tug-of-war between the ligand-field effect and conceivable ferromagnetic interactions between the Dy^{III} ions. The *M vs H/T* (Fig. 6B, inset) data at different temperatures disclose a prompt upsurge of the magnetization at low magnetic fields, which finally reaches a value of 30.9 μ_B at 1.9 K and 7 T devoid of any indication of saturation. The difference between this lower value and the corresponding expected saturation value of 60 μ_B (for six non-interacting Dy^{III} ions), is presumably because of anisotropy and the crystal-field effects at the Dy^{III} ion, which eradicate the 16-fold degeneracy of the $^6H_{15/2}$ ground state. The non-superposition of the *M vs H/T* data on a single master curve refers to the existence of noteworthy magnetic anisotropy and/or low-lying excited states in compound **10**. The dynamics of the magnetization were probed using AC susceptibility measurements, results of which in the zero static field and a 3.0 Oe ac field oscillating at various frequencies from 1 to 1500 Hz are shown in Fig. 6C. At temperatures below ~30 K, a frequency-dependent out-of-phase (χ'') ac signal divulges the onset of slow relaxation of the magnetization, which is a characteristic feature of SMM behavior. The relaxation time was calculated from the frequency-dependent data between 1.9 and 17 K, and the Arrhenius plot obtained from these data is given in Fig. 6D. It is noteworthy that two relaxation regimes are quite prominently evident, which might be ascribed to single-ion relaxation of individual Dy^{III} ions and the weak coupling between each of them at high and low temperatures, respectively.

In efforts to craft novel polynuclear lanthanide clusters showing slow relaxation of magnetization, Tang *et al.* achieved an unparalleled hexanuclear dysprosium cluster (**11**) (Ke *et al.,* 2011) using 1,3-bis(salicylideneamino)-2-propanol (H_3L) as ligand, which was well-recognized as a versatile chelating and bridging group taking part in the formation of quite a few number of 3d metal clusters (Mukherjee *et al.* 2005; Dhara *et al.,* 2007; Lu *et al.,* 2009). Interestingly, from a structural point of view, complex **11** indicated an unprecedented "edge-to-edge" arrangement of two Dy_3 triangles. The reaction of dysprosium nitrate with H_3L in methanol/acetonitrile solvent mixture, in the company of triethylamine, produced this Dy_6 cluster with formula $[Dy_6^{III}(L)_4(\mu_3\text{-}OH)_4(CH_3OH)_2(NO_3)_2]\cdot 6CH_3CN$ (**11**) (presented in Fig. 7A). The $[Dy_6(\mu_2\text{-}O)_6(\mu_3\text{-}OH)_4(\mu_3\text{-}O)_2]^{6+}$ core comprises of two $[Dy_3(\mu_3\text{-}O)(\mu_3\text{-}OH)]$ triangular units in a typical "edge-to-edge" arrangement coupled by two μ_3-OH–ions and two deprotonated alcohol oxygen atoms from two $\eta_1{:}\eta_1{:}\eta_3{:}\eta_3{:}\mu_4\text{-}L^{3-}$ ligands. It is mention-worthy that the topology in complex **1** was quite different from all the previously reported Dy_6 congeners, in which the vertices of two almost parallel triangles were linked through bridging alkoxide oxygen atoms of two ligands, leading to a "head-to-head" arrangement of the dysprosium triangles, in which all the Dy-centres were eight-coordinated. The plot of $\chi_m T$ vs. *T* is shown in Fig. 7B. At 300 K, the $\chi_m T$ value of 83.6 cm^3Kmol^{-1} is markedly close to the anticipated value of 85.0 cm^3Kmol^{-1} for six uncoupled Dy^{III} ions ($S = 5/2$, $L = 5$, $J = 15/2$, $6H_{15/2}$, $g = 4/3$). The value of $\chi_m T$ steadily decreases till 75 K followed by a further decrease to 56.6 cm^3Kmol^{-1} at 2 K, which may credibly be ascribed to a combination of the progressive depopulation of the excited Stark sublevels and the expected exchange interactions between the Dy^{III} ions. The non-superimposition of the *M vs. H/T* data on a single curve affirms the presence of a noteworthy magnetic anisotropy and/or low-lying excited states. Moreover, the maximum value for magnetization is consistent with the estimated value (6×5.2 μB) for six uncorrelated Dy^{III} ions with a value of 5.2 μ_B for each Dy^{III} ion, taking into account the existence of considerable ligand-field effects. Fig. 7C depicts the dynamics of magnetization by the plots of χ' *vs. T* and χ'' *vs. T*. Compound **11** shows frequency-dependent in-phase (χ') and out-of-phase (χ'') signals, which signify the occurrence of slow magnetic relaxation at low temperature. AC susceptibility measurements as a function of frequency at different temperatures were performed with the resultant plots shown in Fig. 7D. The relaxation time at different temperatures was extracted by fitting the curves χ'' *vs.* frequency. In a nutshell, this report explored the formation of an unprecedented Dy_6 cluster with two edge-to-edge Dy_3 triangles by employing the pentadentate schiff base ligand H_3L in two incongruent binding modes and

its slow magnetic relaxation behavior. The interesting magnetic behavior in such compounds was attributed to the magnetic anisotropy of the molecules, which depends not only on the individually singular anisotropies of the metal ions, rather also on the relative orientation of the local axes.

The Year 2012 came up with three new major discoveries in the Ln_6 domain. While the first one was from Tang *et al.* in March (Guo *et al.,* 2012), followed by one more report from Murray *et al.*, (Langley *et al.*, 2012), the fag end of the year witnessed Chibotaru and Ungur *et al.* put in their collective efforts in one more significant report (Ungur *et al.*, 2012) concerning theoretical studies on the earlier reported Dy_6 wheel compound **3**.

With the objective of elaborating molecular nanoclusters, new attempts to connect magnetic Dy_2 building blocks into larger molecules were performed by Tang *et al.* the use of the carbonato ligand(s) with potential coordination modes. When carbonate was purposefully introduced to Dy^{III} and vanillin picolinoylhydrazone (H_2ovph) reaction mixture in the presence of triethylamine, they effectively lead to a hexanuclear complex, $[Dy_6(ovph)_4(Hpvph)_2Cl_4(H_2O)_2\text{-}(CO_3)_2]\cdot CH_3OH\cdot H_2O\cdot CH_3CN$ (**12**), with a triangular prism arrangement. Notably, crystals of complex **12** were formed by the direct feeding of CO_2, whereas crystals of an octanuclear complex, $[Dy_8(ovph)_8(CO_3)_4\text{-}(H_2O)_8]\cdot 12CH_3CN\cdot 6H_2O$ (**13**), with a tub conformation, assembled in the presence

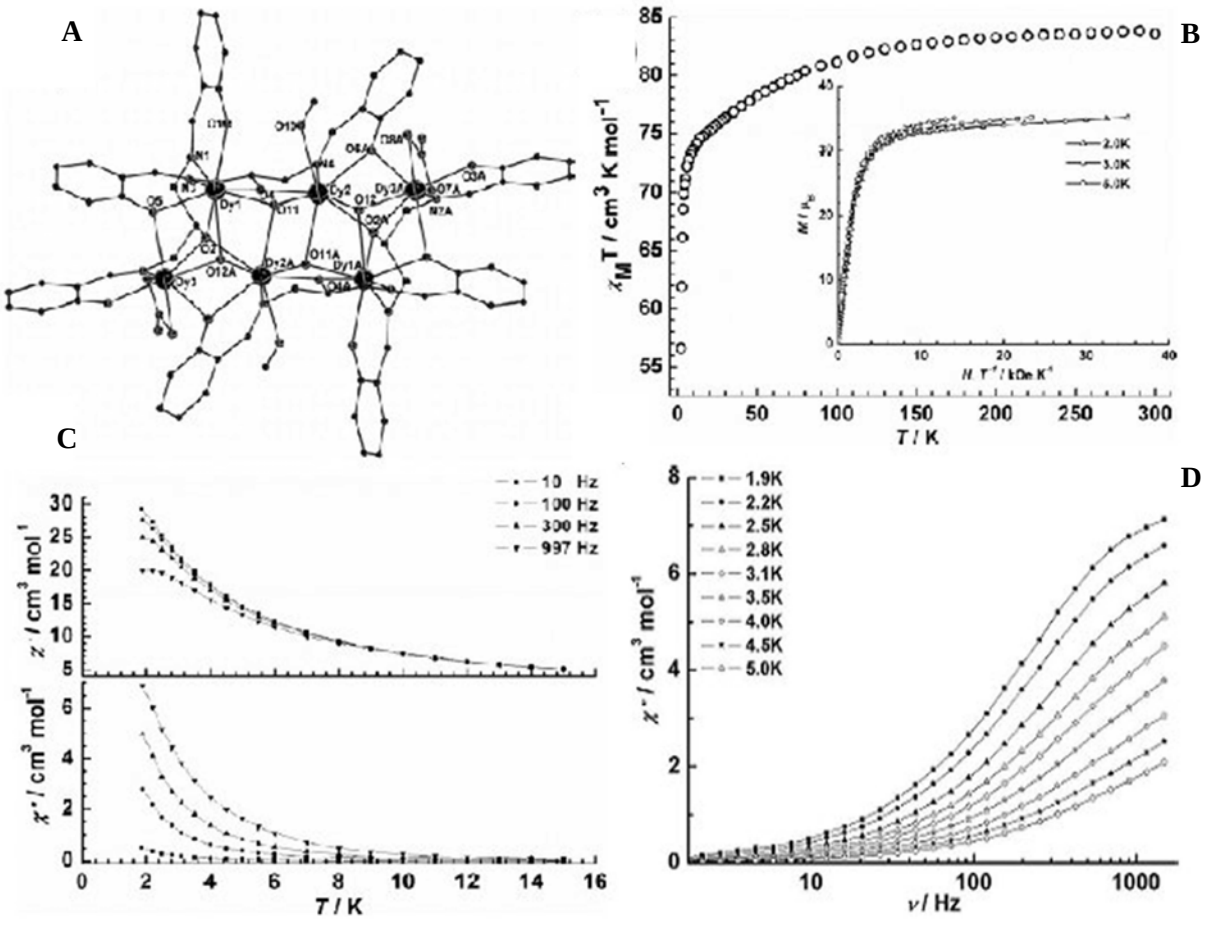

Fig. 7: (A): Molecular structure of complex 11. H atoms are omitted for clarity; (B): Temperature dependence of the $\chi_m T$ product at 1 kOe. Inset: *M vs H/T* plots at different temperatures below 5 K for complex 11; (C): Temperature dependence of in-phase (top) and out-of-phase (bottom) ac susceptibility components at different frequencies and zero applied dc field for complex 11; (D): Frequency dependence of out-of-phase ac susceptibility of complex 11. [Reprinted with permission from Ref. Ke *et al.,* 2011. Copyright (2011) Wiley-VCH]

of sodium carbonate. After the static and dynamic magnetic properties were comprehensively studied, it was found that in the Dy_6 aggregate (**12**), three of the constituent Dy_2 "skeletons", having been well conserved, contribute to the overall SMM behavior with a reasonably slow tunneling rate, while the Dy_8 cluster (**13**) only exhibits a rather small relaxation barrier. The discussion herein will simply focus on the hexanuclear compound **12**. The reaction of $DyCl_3$ with H_2ovph in the binary solvent mixture of methanol/acetonitrile in presence of base triethylamine, by feeding CO_2, produces the Dy_6 cluster **12**, whose molecular structure is represented in Figs. 8A and B. The Dy_6 structure can be considered as one resulting from the formal linkage of two carbonato ligands from three petals of the Dy_2 units, with the concomitant formal loss of the terminal ligands. The direct-current (dc) magnetic susceptibility of complex **12** has been measured in an applied magnetic field of 1000 Oe in the temperature range 300-2 K and can be seen plotted as $\chi_m T$ *vs* T in Fig. 8C. The $\chi_m T$ value at 300 K of 82.1 cm^3 K mol^{-1} is lesser than the predictable value of 85.02 cm^3 K mol^{-1} for six uncoupled Dy^{III} ions (S = 5/2, L = 5, $^6H_{15/2}$, and g = 4/3), and it gradually decreases with declining temperature until 20 K. Thereafter a small maximum was observed as the temperature fell further (75.3 cm^3 K mol^{-1} at 6 K), before a further brisk fall at the lowest temperature was noted. The Stark sublevels of the anisotropic Dy^{III} ions remain thermally depopulated when the temperature got lowered; ensuing in a reduction of the $\chi_m T$ product at the high-temperature range, and the maximum is possibly due to the existence of an intramolecular ferromagnetic interaction involving the metal ions. A residual slope is observed at high field (>60 kOe) on the *M vs H* data (inset of Fig. 8C), indicating incomplete saturation of the magnetization and the simultaneous existence of some anisotropy and/or low-lying excited states in the concerned hexanuclear system. The dynamics of the magnetization were investigated using alternating-current (ac) susceptibility measurements, with the outcome in zero static field given in Fig. 8D. Each $\chi' T$ value exhibits an abrupt decrease with diminishing T depending on the ac frequency, signaling the "freezing" of the spins by the anisotropy barrier. This is accompanied by a frequency-dependent out-of-phase (χ'') signal. In the bottom panel of Fig. 8D, the χ'' curves were divided by the dc susceptibility χ_{dc}, so that the relaxation time τ matches the inverse of the angular frequency ω just at the peak temperature of the corresponding curve, where the $\chi' T$ dispersion curve is observed. χ''/χ_{dc} signal is seen with a maximum at 15 K for 1000 Hz, which shifts to the low-temperature regime as the frequencies drop down to 1 Hz. All of these features are pinpointing to the slow relaxation of the molecular magnetization and, consequently of SMM behavior. The magnetization relaxation time (τ) can be derived from the temperature (Fig. 8D) and plotted as a function of *1/T* in Fig. 8E. The resultant nature of the plot, characteristic of the magnetic behaviour of the material is indicative of a crossover from a thermally activated Orbach mechanism predominant at high temperature to a quantum tunneling relaxation pathway at T < 10 K. At lower temperature, the exchange interaction between the metal sites is a crucial factor for blockage of the magnetization in the weak exchange limit, which may cause a relatively slow tunneling rate (>0.2 s). The data plotted as Cole-Cole plots present a perfectly symmetrical shape (Fig. 8F), which is chiefly useful to measure the width distribution of the relaxation rate by introducing the α parameter in the Debye formula (α = 0 for a Debye model). Such a symmetrical shape is noteworthy, because lanthanide systems frequently provide a very broad distribution or an asymmetrical Cole-Cole plot, in the low-temperature regime, while **12** showed a narrow distribution along with a moderate increase of the dispersion upon lowering T. Therefore, the dominance of a single relaxation process agrees with the presence of a unique coordination sphere of Dy^{III} ion in **12**. In summary, three well preserved Dy_2 "skeletons" linked by two carbonato ligands, forming a triangular prism arrangement contribute to the SMM behavior of compound **12** with a reasonably slow tunneling rate. It was experimentally verified that the employment of highly axial single lanthanide building blocks is an expedient strategy for the design of molecular architectures with the appropriate structure to further utilize their functional properties.Murray

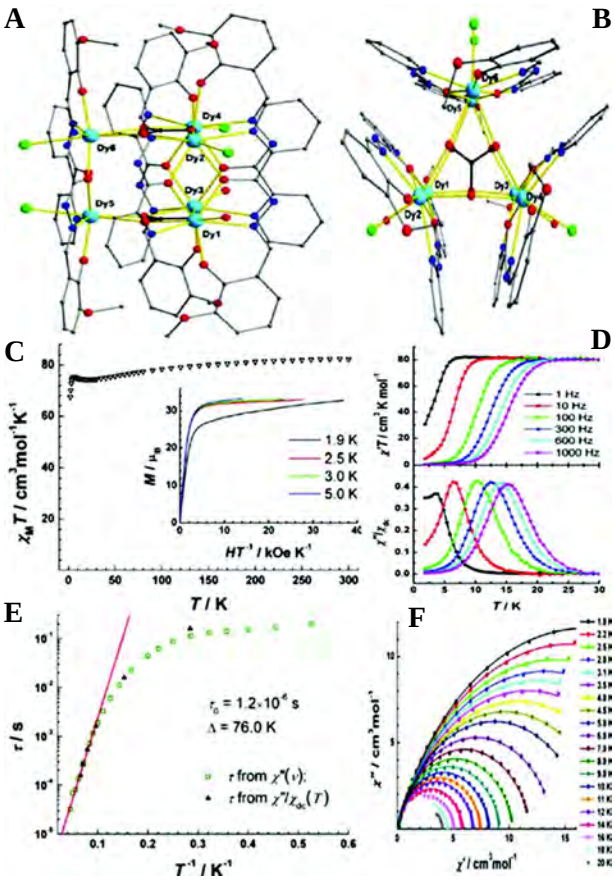

Fig. 8: (A): Side view of complex 13, B: top view of the molecular structure of complex 13; H atoms are omitted for clarity; scheme: sky blue, Dy; red, O; blue, N; green, Cl; gray, C; (C): Temperature dependence of the $\chi_m T$ product at 1000 Oe and field dependence of the magnetization at low temperatures (inset) for complex 13; (D): Temperature dependence of the ac magnetic susceptibility for complex 13 of the imaginary component (bottom) and $\chi' T$ product (top) in zero static field. The χ'' data are normalized at each temperature by the corresponding value of χ_{dc}; (E): Magnetization relaxation time τ versus T^{-1} plot for 13 under zero dc field. The line is fitted with the Arrhenius law; (F): Cole-Cole plots measured below 20 K and zero dc field. The lines represent the best-fit calculated values for each temperature with an extended Debye model with α parameters below 0.23. [Reprinted with permission from Ref. Guo *et al.*, 2012. Copyright (2012) American Chemical Society]

and co-workers adopted a mixed-ligand approach by performing reactions with the use of $teaH_3$ (triethanolamine) along with coligand Hchp (6-chloro-2-hydroxypyridine) (Langley *et al.*, 2012). The reaction of $Ln(NO_3)_3 \cdot 6H_2O$ (Ln = Gd, Tb, and Dy), $teaH_3$, and Hchp in a methanolic solution led to the formation of colorless plate-shaped crystals after slow evaporation over a brief period, which resulted in three novel isostructural hexanuclear lanthanide clusters of the general formula $[Ln^{III}_6(teaH)_2(teaH_2)_2(CO_3)(NO_3)_2(chp)_7(H_2O)](NO_3) \cdot 4.5MeOH \cdot 1.5H_2O$ [Ln = Gd (**14**), Tb (**15**), and Dy (**16**)]. Compounds **14-16** (compound **16** is shown in Fig. 9A) crystallize in the triclinic space group P1, with the entire cluster as its asymmetric unit, as well as a nitrate counterion and MeOH and H_2O solvent molecules. Each cluster is isostructural, and only compound **16** (Dy_6) will be discussed here. The complex consists of six Dy^{III} ions, with the metallic core displaying an unusual motif. The best description of it would be as four coplanar Dy^{III} ions (Dy1, Dy4, Dy5, and Dy6) forming a trapezoid, with the residual two metal ions (Dy_2 and Dy_3) lying above and below the plane of the longest rectangular edge (Fig. 9B). It was observed that at the center of the Dy_6 core a carbonate ion is present, which adopts a μ_6:η_2:η_2:η_2-bonding mode, binding to all metal ions present, and it seems to be directing the positions of these ions. The conversion of CO_2 to CO_3^{2-} may be similar to the mechanism of carbonic anhydrase. In this instance, it invokes the nucleophilic attack of hydroxo species bound to the Ln ions in basic conditions to the electrophilic C atom of CO_2. This, then remains bound to the metal ion, and it is apparent that the carbonate core emerges significant in the formation and subsequent isolation of the cluster. Direct-current (dc) magnetic susceptibility measurements were done on polycrystalline samples of **14-16**, in the 300-2 K temperature range, and in applied magnetic fields of 1, 0.1, and 0.01 T. Plots of $\chi_m T$ *vs* T are provided in Fig. 9C. Compound **14** {Gd_6} yields a room temperature $\chi_m T$ value of 42.90 $cm^3\ mol^{-1}\ K$, which is consistent with the presence of six non-interacting (S = 7/2) centers (47.25 $cm^3\ mol^{-1}\ K$; g = 2). The values remain unaltered upon a decrease of the temperature to ~10 K, below which a sharp decrease is noted, with a value of 23.34 $cm^3\ mol^{-1}\ K$ found at 2 K, in the field 1 T. There is no field dependence in $\chi_m T$ below 70 K. The data imply that weak intracluster antiferromagnetic coupling is occurring. The $\chi_m T$ values gradually decrease upon lowering of the temperature, before a more sudden decline below 10 K. This is because of depopulation of the m_J sublevels

of the *J* ground state and probably weak antiferromagnetic interactions. Plots of χ_m'' *vs T* for complex **16** are shown in Fig. 4. The out-of-phase susceptibility (χ_m'') exhibits frequency-dependent "tails" at low temperatures for all the compounds, which is evocative of the existence of slow relaxation of the magnetization, typical of SMM behavior. Summing it up, a new hexanuclear cluster type for lanthanide compounds had been primed by the assembly of Ln ions and the ligands $teaH_3$ and Hchp, in which the cluster core contained a μ_6-carbonate ligand, derived from atmospheric CO_2 fixation. Magnetic studies revealed weak coupling and antiferromagnetic interactions for compound **14** {Gd_6}. Compounds **15** {Tb_6} and **16** {Dy_6} display characteristic features of SMM materials.

From theoretical standpoint, Chibotaru and Ungur *et al.* described a toroidal magnetic moment in the absence of conventional total magnetic moment for a well-known Dy_6 ring compound **3** (Ungur *et al.*, 2012), reported by Murray *et al.* (Langley *et al.*, 2010) in 2010. The importance of their work lied in the fact that, in distinction to all the known Ln_6 compounds from the literature, this Dy_6 complex owed its net toroidal magnetic moment to high rotational symmetry. According to the extensive magnetic study, the rationale for the net toroidal arrangement of the local magnetic moments could be ascribed to the high symmetry of the complex and strong intramolecular dipolar interactions between Dy ions. The portrayal of single-ion and inter-ion anisotropic magnetic interactions is accomplished here for the first time entirely *ab initio*, i.e., devoid of the use of phenomenological parameters. Since this review is intended to discuss the Ln_6 complexes from the aspects of structural viewpoint and synthetic strategies, neither of which typically relate to theoretical studies, we abstain from the detailed discussion of this theoretical report. Although a clear mention of the important conclusive finding from the detailed *ab initio* investigation for the electronic and magnetic structure of the Dy_6 wheel should be made here. The revelations clearly suggested that the obtained strong stabilization of toroidal magnetic moment allows for its experimental observation.

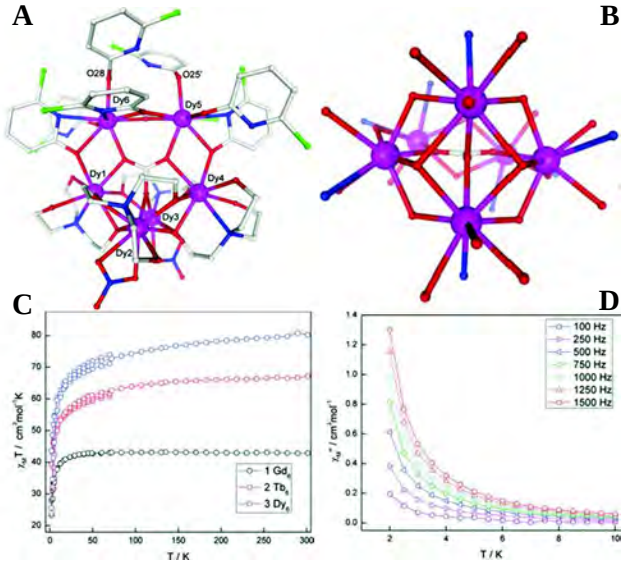

Fig. 9: (A): Molecular structure of complex 16. H atoms and solvent molecules are omitted for clarity; (B): Side view of compounds 14-16; (C): Plots of $\chi_m T$ *vs T* for complexes 14 **(bottom), 15 (middle), and 16 (top) measured at 1 T (2-300 K) and 0.1 and 0.01 T (2-70 K); (D) Plot of χ_m'' *vs T* for complex 16. H_{dc} = 0. [Reprinted with permission from Ref. Langley *et al.*, 2012. Copyright (2012) American Chemical Society]**

The last year, 2013, registered two vital reports in the Ln_6 domain. Thompson *et al.* started with the discovery of a new kind of hexanuclear Ln_6 complexes [complexes **17** (Gd), **18** (Tb) and **19** (Dy)], along with new Ln-complexes of varying nuclearity (mono, di- and tri- and tetra) (Anwar *et al.*, 2013). This was done by exploiting the fascinating lanthanide coordination chemistry of a tri-functional vanillin-hydrazone-oxime based ligand, which led to different complexes with varying nuclearity depending on reaction conditions. As a matter of fact, these Ln_6 complexes are formed in the presence of both triethylamine and acetic acid, and have flat, unique hexanuclear structures built on a μ_3-O bridged triangular core, with the six lanthanide ions bridged additionally via μ-acetate and μ-$O_{hydrazone}$ links in an expanded fused triangular array. Firstly, the examples of *o*-vanillin based $Dy^{(III)}$ clusters especially suitable for exhibiting slow magnetic relaxation and possible SMM behaviour became quite well-known. Taking into account the fact that the triangular arrays are usually formed by oxime groups, and considering the verified self-assembly of $Ln^{(III)}$ ions with hydrazone based ligands, the authors decided to examine the

lanthanide coordination chemistry of a ligand (1Z,2E)-N-((E)-1-(2-hydroxy-3-methoxyphenyl) ethylidene)-2-(hydroxyimino)propanehydrazonic acid to see whether similar directed assembly patterns are observed, and which of the functional groups contribute to the cluster product. Reactions of ligand with Ln(III) (Ln = Gd, Tb, Dy) formed a exclusive series of $Ln(III)_6$ clusters with an absolutely fused and highly symmetric triangular motif in the complexes $[(L_6\text{-}2H)_6Ln_6(O)(CH_3COO)_6]$ (Ln = Gd (**17**), Tb (**18**), Dy (**19**)), evocative of a fragment of an edge- fused triangular lattice. Six ligands cover the entire Ln_6 cluster largely by hydrazone (μ-O) bridging. Complexes **17**-**19** are produced as pale yellow crystals by the reaction of the participating ligand with $Ln(NO_3)_3$, in the simultaneous presence of acetic acid and triethylamine. The participating ligand possesses three potentially ionizable protons, with the phenolic and hydrazone OH protons anticipated to be the most acidic in the ambience of a metal and the additional triethylamine.

All the structures **17**-**19** disclose a complex stoichiometry with six Ln(III) ions (Ln = Gd, Tb, Dy), six acetates along with a central μ_3-O atom, nominally designated as oxide. The molecular structure of the Gd_6 cluster in **17** is shown in Fig. 10A, and the abbreviated structural core highlighting the immediate donor atoms in Fig. 10B. Analogous representations for complexes **18** and **19** are demonstrated in Figs. 10C, D and E, 10F respectively. Six ligands encompass the edges of the overall triangular arrangement binding all the way through hydrazone oxygen and nitrogen atoms, oxime nitrogen and vanillin phenolic oxygen atoms. One core bridging element involves the hydrazone oxygens from each of the six ligands, which lead to bridges between the Gd ions on the periphery of the molecular triangle. Additional oxygen bridges from six η_3–μ_2-O acetate groups connect the Gd ions within each corner triangle, and a μ_3-O 'oxide' completes the bridging in the central triangle. The inconsistent coordination motifs seen within the group of lanthanide ions studied with the ligand is conceivably not unanticipated, considering the choice of donor groups involved, counting the coligands, and the 'flexible' coordination geometries generally exhibited

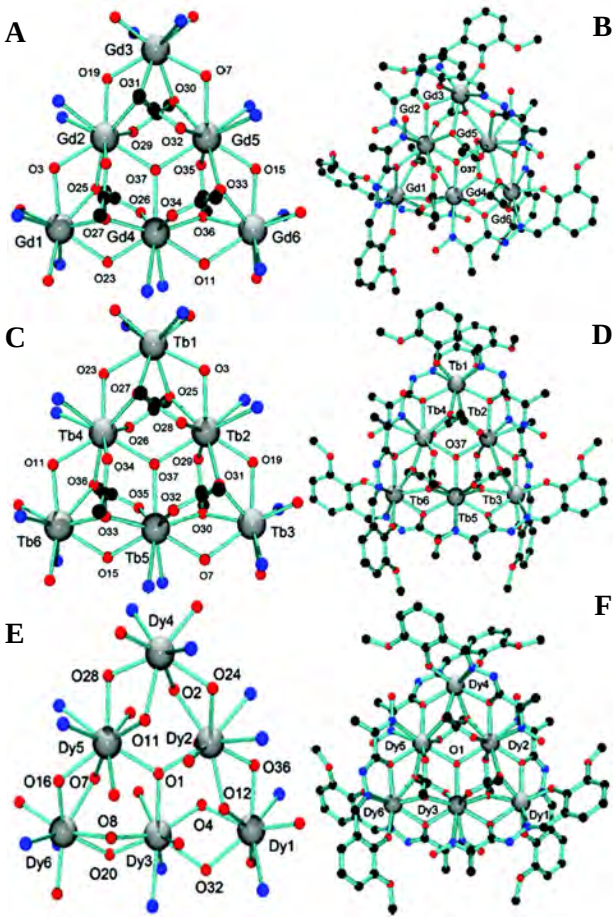

Fig. 10: (A): Core structural representation of complex 17; (B): Structural representation of complex 17; (C): Core structural representation of complex 18; (D): Structural representation of complex 18; (E): Core structural representation of complex 19; (F): Structural representation of complex 19. (Anwar *et al.*, 2013)

by these ions. However, the formation of the Ln_6 super-triangles with Gd, Tb and Dy and not with Tm and Yb quite indicatively suggest that ionic radius plays some important role [Ln(III) (in pm); Gd (93.8), Tb (92.3), Dy (91.2), Tm (88.0), Yb (86.8)], since each of the Gd(III), Tb(III) and Dy(III) ions possesses notably superior radii than Tm, Yb.

Variable temperature dc susceptibility data (0.1 T field) expressed as $\chi_m T$ per mole for complexes **17**–**19** are presented in Fig. 11. The room temperature χT value of 48.0 cm^3 K mol^{-1} for **17** is a little higher than the theoretical value of 47.3 cm^3 K mol^{-1} calculated for six non-interacting Gd(III) ions (S = 7/2, L = 0, $^8S_{1/2}$, g = 2). As the temperature declines,

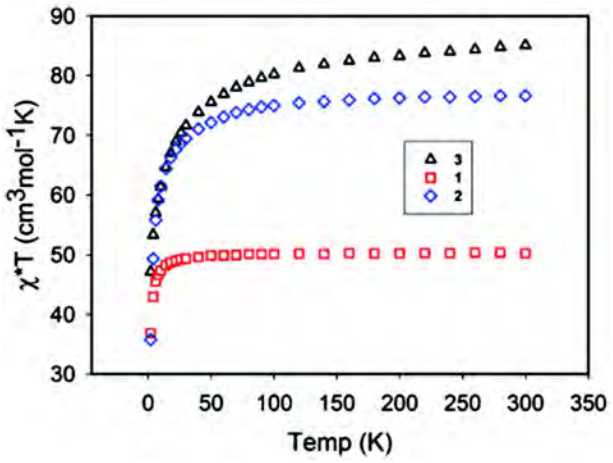

Fig. 11: Variable temperature DC magnetic data for complexes 17-19. (Anwar *et al.*, 2013)

the χT values drop down to some extent, approximately 50 K followed by a more rapid decrease to 2.0 K, attaining a value of 35.2 cm^3 K mol^{-1}. Considering the usual isotropic character of Gd(III), and the lack of any noteworthy orbital contribution to its magnetic properties, the observed minute drop in χT on lowering temperature is reasonably linked with intramolecular antiferromagnetic exchange. Similar results are obtained for the other two Ln_6 systems also, namely Tb_6 and Dy_6, which are equivocally suggestive of magneto-anisotropy, and/or the presence of low lying excited states. AC measurements even below 2 K show no significant out of phase frequency or field dependent signals, suggesting the absence of any SMM behaviour.

To summarize the findings of this particular report, the involved multi-functional ligand, with vanillin, hydrazone and oxime groups, forms a series of exclusive flat and fused triangular Ln_6 complexes (Ln = Gd, Tb, Dy), with hydrazone O atoms linking the Ln centers, in addition to a μ_3 central 'oxide', and six bidentate bridging acetates. The vanillin OMe and oxime OH groups stay uncoordinated. Intramolecular antiferromagnetic coupling is seen in the Gd_6 case, while the Dy_6 and Tb_6 complexes have trivial out of phase AC signals down to 2 K, indicating the lack of SMM behavior.

Last such report on a Ln_6 molecular nanomagnet came from Ghosh *et al.*, which dealt with the synthesis, characterization and magnetic studies over a novel hexanuclear dysprosium(III) cluster $[Dy_6(L)_7(HL)(MeOH)_2(H_2O)(OH)_2(OAc)]$ (**20**) (Mukherjee *et al.*, 2013). This complex was synthesized from the well-known π-conjugated Schiff base ligand H_2L, namely, *o*-phenolsalicylimine (comprising of two similar proximate pockets for metal-coordination, Fig. 12A) and dysprosium nitrate. This unique Dy^{III}_6 cluster, formed by the exclusive combination of two vertex-sharing and one edge-sharing high-anisotropy Dy_3 triangles (Fig. 12E) gives rise to an unprecedentedly asymmetric Dy^{III}_6 homometallic core, which exhibits slow magnetic relaxation. A perspective view of the hexanuclear Dy^{III} complex is represented in Fig. 12B. Among eight of the ligands in the molecule, seven are completely deprotonated while the eighth one still remains protonated. The ligands coordinated by each of their two oxygen donor sites and the central nitrogen site are building one five membered and one six membered chelating ring with the Dy centers. L is coordinated in bridging plus chelating modes, where none of the metal centers are bridged by central nitrogen, but associated by their termini's containing phenoxo groups. Abridgment of the structural aspects reflect that each of the Dy_6 unit, composed of the fusion of three triangular Dy_3 subunits (A, B and C, Fig. 12E), formally also involves an edge-sharing Dy_4 block (Fig. 12E), defined by Dy_3, Dy_4, Dy_5 and Dy_6), which again couples to two more Dy-centers (Dy_1 and Dy2) to constitute the overall asymmetric Dy_6 unit.

Direct current (dc) magnetic susceptibility studies of a polycrystalline sample (Fig. 12D) reveal a room-temperature $\chi_m T$ value equal to 82.39 cm^3 K mol^{-1}, approaching the expected value for six uncoupled Dy^{III} ions (C = 14.17 cm^3 K mol^{-1}). The $\chi_m T$ values get reduced gradually with diminishing temperature. This may plausibly be ascribed to a conceivable blend of the progressive depopulation of excited Stark sublevels and likely exchange interaction between the Dy^{III} ions. The *M* versus *H* data at different temperatures demonstrate a swift rise in the magnetization at low fields, reaching values of 32.09 μB at 1.9 K and 7 T for Dy_6 (Fig. 12F). The

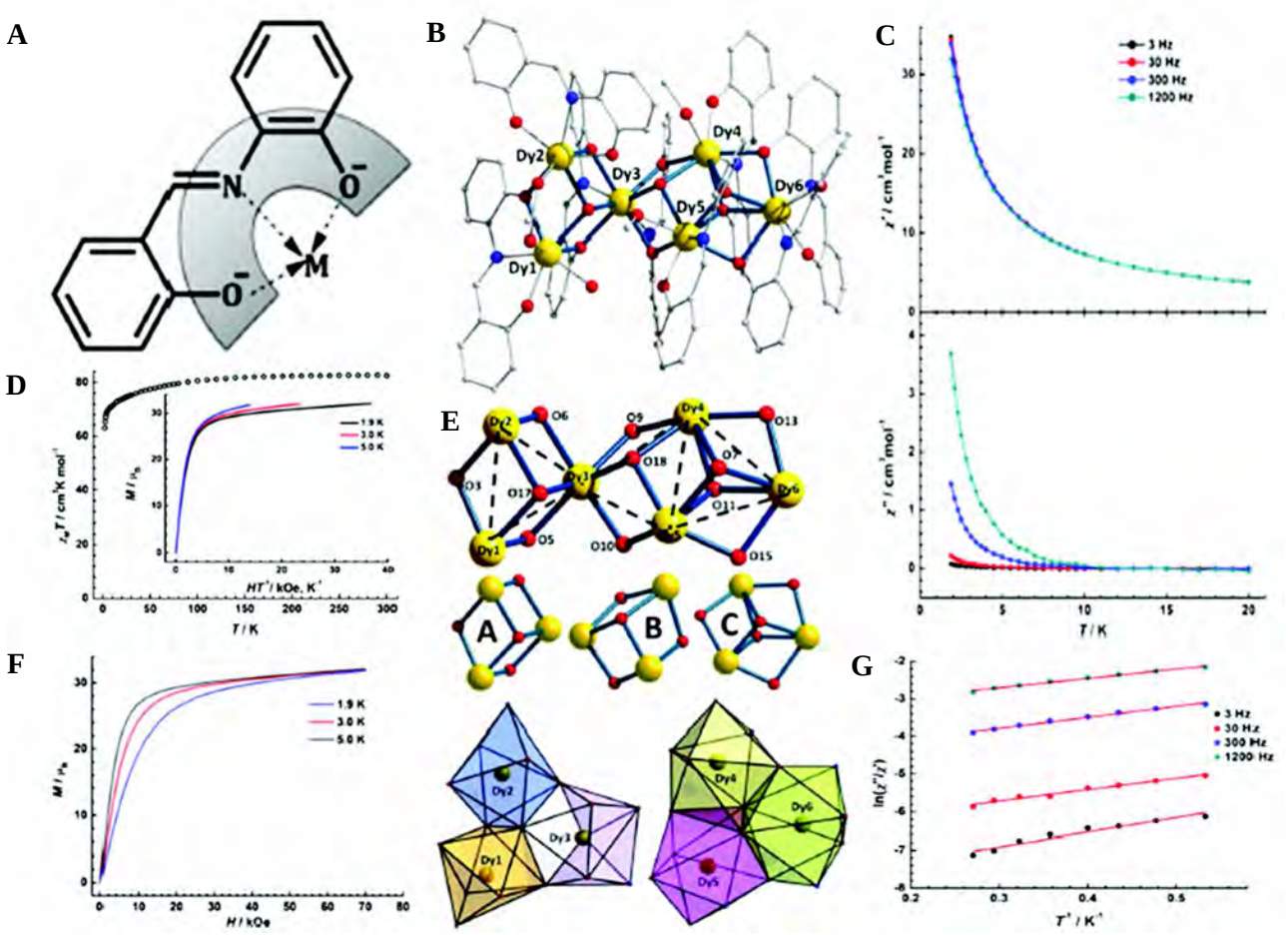

Fig. 12. (A): Structure of the deprotonated ligand L with M (M = Dysprosium) fitting in the pocket; (B): Hexanuclear unit of 20 with the central core highlighted by blue bonds. H atoms are omitted for clarity. Color scheme: yellow, Dy; red, O; blue, N; (C): Temperature-dependent ac susceptibility data for compound 20, collected under zero dc field at the indicated frequency; (D): Temperature dependence of $\chi_M T$ at 1 kOe for 1 (with $\chi = M / H$ normalized per mol). Inset: M vs. H / T plot at various temperatures between 1.9 and 5 K; (E): Top: Asymmetric central metal core of Dy_6 unit in 20 bridged by oxygen atoms displaying the three fused triangular units shown by the dashed black lines, Middle: The triangular subunits A, B and C shown separately; subunits A and B being similar to each other but, different from the subunit C, Bottom: Coordination polyhedra of six distorted Dy-centers shown in different colors. structure of 20. H atoms and solvent molecules are omitted for clarity; (F): Field dependence of the magnetization at various temperatures between 1.9 and 5 K; G: Natural logarithm of the ratio of χ'' over χ' versus $1 / T$ of the data for 20 given in Fig. 12C [Reprinted with permission [Mukherjee *et al.*, 2013. Copyright (2013) with permission from Elsevier]

non-superimposed curves validate the presence of anisotropy and/or low-lying excited states. The dynamics of the magnetization measurements operating in a 3.0 Oe ac field oscillating at the indicated frequencies (3-1200 Hz) and with a zero-dc field for Dy_6 is shown in Fig. 12C, as the plots of χ' vs. T and χ'' vs. T. To approximately evaluate the energy barrier U_{eff} and τ_0, another method which was proved to be successful in the determination of energy barriers for Mn_{12}, Dy_2 or $[Dy_4(\mu_3\text{-}OH)_4]^{8+}$ cubane based systems was employed. Based on the assumption that there is a single characteristic relaxation process of the Debye type with only one energy barrier and one time constant, the following relation (eq.) is obeyed: $\ln(\chi''/\chi') = \ln(\omega\tau) + U_{eff} / kT$. As shown in Fig. 12, linear fitting of the experimental $\ln(\chi''/\chi')$ data to the said equation leads to the parameters $U_{eff} \approx 3.0$ K and $\tau_0 \approx 8.3 \times 10^{-6}$ s. The frequency-dependent out-of-phase signals were observed, signifying the onset of slow magnetization

relaxation. The absence of frequency-dependent peaks in the out-of-phase susceptibility signals for this Dy_6 system was most likely attributed due to the fast quantum tunneling of the magnetization.

Conclusion

The huge upsurge in the number of recent publications based on molecular magnets is undoubtedly a strong indication of the progressively escalating interest that has developed, looking for the more appropriate novel strategic designs of the molecular magnets, which in a way, can develop smart functional SMMs with excellent properties suitable from application-perspectives. Several examples have made it evident that lanthanide elements, especially Dysprosium, display the superiority in magnetism over the transition metals as an outcome of their ground states with highly anisotropic angular momentum. Therefore, Dy-based high-nuclearity SMMs are potential candidates for the development of next-generation molecular magnet species. Considering these facts, the systematic study of the magnetically intriguing Ln_6 molecules, as done by various research groups over the last five years, since the breakthrough discovery in 2009, have been summarized here from the various aspects of structural overview and synthetic approaches.

Future Prospects

As a concluding synopsis of this discussion, it seems quite judicious to point out that only a combined input of the experimental efforts like these mentioned Ln_6 reports, coupled with theoretical calculations and doping studies, should turn out crucial in the near future to realize the underlying fundamental mechanism in polynuclear lanthanide complexes and their structure-property relationships, which in effect should open new avenues for investigating the relaxation dynamics of lanthanide aggregates.

Acknowledgements

We thank IISER Pune for research facilities and funding. DAE (Project No.2011/20/37C/06/BRNS) is also acknowledged for the financial support.

References

Abragam A and Bleaney B (2012) Electron Paramagnetic Resonance of Transition Ions. Oxford University Press, New York. (53) Morrish A H (1966) The Physical Principles of Magnetism. Wiley, New York

Anwar M U, Dawe L N, Tandon S S, Bunge S D and Thompson L K (2013) Polynuclear lanthanide (Ln) complexes of a tri-functional hydrazone ligand-mononuclear (Dy), dinuclear (Yb, Tm), tetranuclear (Gd), and hexanuclear (Gd, Dy, Tb) examples *Dalton Trans* **42** 7781-7794

Anwar M U, Tandon S S, Dawe L N, Habib F, Murugesu M and Thompson L K (2012) Lanthanide Complexes of Tritopic Bis(hydrazone) Ligands: Single- Molecule Magnet Behavior in a Linear Dy^{III}_3 Complex *Inorg Chem* **51** 1028-1034

AlDamen M A, Clemente-Juan J M, Coronado E, Martí-Gastaldo C and Gaita-Arino A (2008) Mononuclear Lanthanide Single-Molecule Magnets Based on Polyoxometalates *J Am Chem Soc* **130** 8874-8875

Ardavan A, Rival O, Morton J J L, Blundell S J, Tyryshkin A M, Timco G A and Winpenny R E P (2007) Will Spin-Relaxation Times in Molecular Magnets Permit Quantum Information Processing? *Phys Rev Lett* **98** 057201-1-057201-4

Bogani L and Wernsdorfer W (2008) Molecular spintronics using single-molecule magnets *Nat Mater* **7** 179-186

Boskovic C, Brechin E K, Streib W E, Folting K, Bollinger J C, Hendrickson D N and Christou G (2002) Single-Molecule Magnets: A New Family of Mn_{12} Clusters of Formula $[Mn_{12}O_8X_4(O_2CPh)_8L_6]$ *J Am Chem Soc* **124** 3725-3736

Bouchiat V, Wernsdorfer W and Balestro F (2008) Quantum phase transition in a single-molecule quantum dot *Nature* **453** 633-637

Brechin E K, Boskovic C, Wernsdorfer W, Yoo J, Yamaguchi A, Sanudo E C, Concolino T R, Rheingold A L, Ishimoto H, Hendrickson D N and Christou G (2002) Quantum Tunneling of Magnetization in a New $[Mn_{18}]^{2+}$ Single-Molecule Magnet with S = 13 *J Am Chem Soc* **124** 9710-9711

Burrow C E, Burchell T J, Lin P H, Habib F, Wernsdorfer W, Cleràc R and Murugesu M (2009) Salen-Based $[Zn_2Ln_3]$ Complexes with Fluorescence and Single-Molecule-Magnet Properties *Inorg Chem* **48** 8051-8053

Caneschi A, Gatteschi D, Sessoli R, Barra A L, Brunel L C and Guillot M (1991) Alternating Current Susceptibility, High Field Magnetization, and Millimeter Band EPR Evidence for a Ground S = 10 State in $[Mn_{12}O_{12}(CH_3COO)_{16}(H_2O)_4)_2CH_3COOH{\cdot}4H_2O$ *J Am Chem Soc* **113** 5873-5874

Cardona-Serra S, Clemente-Juan J M, Coronado E, Gaita-Ariño A, Camón A, Evangelisti M, Luis F, Martínez Pérez M J and Sesé J (2012) Lanthanoid Single-Ion Magnets Based on Polyoxometalates with a 5-fold Symmetry: The Series $[LnP_5W_{30}O_{110}]^{12-}$ (Ln^{3+} = Tb, Dy, Ho, Er, Tm and Yb) *J Am Chem Soc* **134** 14982-14990

Chakov N E, Lee S C, Harter A G, Kuhns P L, Reyes A P, Hill S O, Dalal N S, Wernsdorfer W, Abboud K A and Christou G (2006**)** The Properties of the $[Mn_{12}O_{12}(O_2CR)_{16}(H_2O)_4]$ Single-Molecule Magnets in Truly Axial Symmetry: $[Mn_{12}O_{12}(O_2CCH_2Br)_{16}(H_2O)_4]_4CH_2Cl_2$ *J Am Chem Soc* **128** 6975-6989

Chakraborty A, Ghosh B K, -Arino J R, Ribas J and Maji T K (2012) A Heterometallic (Ni^{II}-Cu^{II}) Decanuclear Cluster Containing Two Distorted Cubane-like Pentanuclear Cores: Synthesis, Structure, and Magnetic Properties *Inorg Chem* **51** 6440-6442

Charalambous M, Moushi E E, Papatriantafyllopoulou C, Wernsdorfer W, Nastopoulos V, Christou G and Tasiopoulos A J (2012) A $Mn_{36}Ni_4$ 'loop-of-loops-and-supertetrahedra' aggregate possessing a high $S_T = 26 \pm 1$ spin ground state *Chem Commun* **48** 5410-5412

Chen P, Chen H, Yan P, Wang Y and Li G (2011) Effect of lanthanide contraction and rigid ligand on the structure of salen-type lanthanide complexes *Cryst Eng Comm* **13** 6237-6242

Chibotaru L, Ungur L and Soncini A (2008) The Origin of Nonmagnetic Kramers Doublets in the Ground State of Dysprosium Triangles: Evidence for a Toroidal Magnetic Moment *Angew Chem Int Ed* **47** 4126-4129

Coronado E and Day P (2004) Magnetic Molecular Conductors *Chem Rev* **104** 5419-5448

Costa J S, Barrios L A, Craig G A, Teat S J, Luis F, Roubeau O, Evangelisti M, Camón A and Aromí G (2012) A molecular $[Mn_{14}]$ coordination cluster featuring two slowly relaxing Nanomagnets *Chem Commun* **48** 1413-1415

Costes J -P, Dahan F and Nicodéme F (2001) A Trinuclear Gadolinium Complex: Structure and Magnetic Properties *Inorg Chem* **40** 5285-5287

Costes J -P, Shova S and Wernsdorfer W (2008) Tetranuclear $[Cu–Ln]_2$ single molecule magnets: synthesis, structural and magnetic studies *Dalton Trans* 1843-1849

Dhara K, Roy P, Ratha J, Manassero M and Banerjee P (2007) Synthesis, crystal structure, magnetic property and DNA cleavage activity of a new terephthalate-bridged tetranuclear copper(II) complex *Polyhedron* **26** 4509-4517

Feng P L, Stephenson C J, Amjad A, Ogawa G, Barco E D and Hendrickson D N (2010) Large Spin-State Changes in Isostructural Cyanate- and Azide-Bridged $Mn_3^{III}Mn_2^{II}$ Single-Molecule Magnets *Inorg Chem* **49** 1304-1306

Gamer M, Lan Y, Roesky P W, Powell A K and Cleràc R (2008) Pentanuclear Dysprosium Hydroxy Cluster Showing Single-Molecule-Magnet Behavior *Inorg Chem* **47** 581-6583

Gatteschi D, Caneschi A, Pardi L and Sessoli R (1994) Large Clusters of Metal Ions: The Transition from Molecular to Bulk Magnets *Science* **265** 1054-1058

Gatteschi D, Sessoli R and Villain J (2006) Molecular Nanomagnets. Oxford University Press, Oxford, UK

Gonidec M, Luis F, Vílchez À, Esquena J, Amabilino D B and Veciana J (2010) A Liquid-Crystalline Single-Molecule Magnet with Variable Magnetic Properties *Angew Chem Int Ed* **49** 1623-1626

Guo Y N, Chen X H, Xue S and Tang J (2012) Molecular Assembly and Magnetic Dynamics of Two Novel Dy_6 and Dy_8 Aggregates *Inorg Chem* **51** 4035-4042

Guo Y N, Xu G F, Gamez P, Zhao L, Lin S Y, Deng R, Tang J and Zhang H J (2010) Two-Step Relaxation in a Linear Tetranuclear Dysprosium(III) Aggregate Showing Single-Molecule Magnet Behavior *J Am Chem Soc* **132** 8538-8539

Guo Y N, Xu G F, Guo Y and Tang J (2011) Relaxation dynamics of dysprosium(III) single molecule magnets *Dalton Trans* **40** 9953-9963

Habib F, Long J, Lin P H, Korobkov I, Ungur L, Wernsdorfer W, Chibotaru L F and Murugesu M (2012) Supramolecular architectures for controlling slow magnetic relaxation in field-induced single-molecule magnets *Chem Sci* **3** 2158-2164

Habib F and Murugesu M (2013) Lessons learned from dinuclear lanthanide nano-magnets *Chem Soc Rev* **42** 3278-3288

Hewitt I J, Lan Y, Anson C E, Luzon J, Sessoli R and Powell A K Opening up a dysprosium triangle by ligand oximation (2009) *Chem Commun* 6765-6767

Hewitt I J, Tang J, Madhu N T, Anson C E, Lan Y, Luzon J, Etienne M, Sessoli R and Powell A K (2010) Coupling Dy_3 Triangles Enhances Their Slow Magnetic Relaxation *Angew Chem Int Ed* **49** 6352-6356

Hussain B, Savard D, Burchell T J, Wernsdorfer W and Murugesu M (2009) Linking high anisotropy Dy_3 triangles to create a Dy_6 single-molecule magnet *Chem Commun* 1100-1102

Ishikawa N, Sugita M, Ishikawa T, Koshihara S and Kaizu Y (2003) Lanthanide Double-Decker Complexes Functioning as Magnets at the Single-Molecular Level *J Am Chem Soc* **125** 8694-8695

Ishikawa N, Mizuno Y, Takamatsu S, Ishikawa T and Koshihara S Y(2008) Effects of Chemically Induced Contraction of a Coordination Polyhedron on the Dynamical Magnetism of Bis(phthalocyaninato)disprosium, a Single-4f-Ionic Single-Molecule Magnet with a Kramers Ground State *Inorg Chem* **47** 10217-10219

Joarder B, Chaudhari A K, Rogez G and Ghosh S K (2012) A carboxylate-based dinuclear dysprosium(III) cluster exhibiting slow magnetic relaxation behaviour *Dalton Trans* **41** 7695-7699

Jiang S D, Wang B W, Sun H L, Wang Z M and Gao S (2011) An Organometallic Single-Ion Magnet *J Am Chem Soc* **133** 4730-4733

Katoh K, Isshiki H, Komeda T and Yamashita M (2012) Molecular Spintronics Based on Single-Molecule Magnets Composed of Multiple-Decker Phthalocyaninato Terbium(III) Complex *Chem Asian J* **7** 1154-1169

Ke H, Zhao L, Guo Y and Tang J (2011) A Dy_6 Cluster Displays Slow Magnetic Relaxation with an Edge-to-Edge Arrangement of Two Dy_3 Triangles *Eur J Inorg Chem* 4153-4156

King P, Wernsdorfer W, Abboud K A and Christou G (2004) A Family of Mn_{16} Single-Molecule Magnets from a Reductive Aggregation Route *Inorg Chem* **43** 7315-7323

Kotzabasaki V, Inglis R, Siczek M, Lis T, Brechin E K and Milios C J (2011) Hexametallic manganese clusters with bulky derivatised salicylaldoximes *Dalton Trans* **40** 1693-1699

Langley S K, Moubaraki B, Forsyth C M, Gass I A and Murray K S (2010) Structure and magnetism of new lanthanide 6-wheel compounds utilizing triethanolamine as a stabilizing ligand *Dalton Trans* **39** 1705-1708

Langley S K, Moubaraki B and Murray K S (2012) Magnetic Properties of Hexanuclear Lanthanide(III) Clusters Incorporating a Central μ_6-Carbonate Ligand Derived from Atmospheric CO_2 Fixation *Inorg Chem* **51** 3947-3949

Leuenberger M N and Loss D (2001) Quantum computing in molecular magnets in *Nature* **410** 789-793

Lin P -H, Burchell T J, Clérac R and Murugesu M (2008) Dinuclear Dysprosium(III) Single-Molecule Magnets with a Large Anisotropic Barrier *Angew Chem Int Ed* **47** 8848-8851

Lin P H, Burchell T J, Ungur L, Chibotaru L F, Wernsdorfer W and Murugesu M (2009) A Polynuclear Lanthanide Single-Molecule Magnet with a Record Anisotropic Barrier *Angew Chem Int Ed* **48** 9489-9492

Lin S Y, Wernsdorfer W, Ungur L, Powell A K, Guo Y N, Tang J, Zhao L, Chibotaru L F and Zhang H J (2012) Coupling Dy3 Triangles to Maximize the Toroidal Moment *Angew Chem Int Ed* **51** 12767-12771

Long J, Habib F, Lin P H, Korobkov I, Enright G, Ungur L, Wernsdorfer W, Chibotaru L F and Murugesu M (2011) Single-Molecule Magnet Behavior for an Antiferromagnetically Superexchange-Coupled Dinuclear Dysprosium(III) Complex *J Am Chem Soc* **133** 5319-5328

Lu J W, Chen C Y, Kao M C, Cheng C M and Wei H H (2009) Synthesis, crystal structure, and magnetic properties of ì-phenoxo/μ-carboxylato-bridged trinuclear nickel(II) complexes with Schiff base, dmf, and urea ligands *J Mol Struct* **936** 228-233

Luzon J, Bernot K, Hewitt I J, Anson C. E, Powell A K and Sessoli R (2008) Spin Chirality in a Molecular Dysprosium Triangle: The Archetype of the Noncollinear Ising Model *Phys Rev Lett* **100** 247205-1-247205-4

Magnani N, Colineau E, Eloirdi R, Griveau J C, Caciuffo R, Cornet S M, May I, Sharrad C A, Collison D and Winpenny R E P (2010) Superexchange Coupling and Slow Magnetic Relaxation in a Transuranium Polymetallic Complex *Phys Rev Lett* **104**, 197202-1-197202-4

Mannini M, Pineider F, Danieli C, Totti F, Sorace L, Sainctavit P, Arrio M A, Otero E, Joly L, Cezar J C, Cornia A and Sessoli R (2010) Quantum tunnelling of the magnetization in a monolayer of oriented single-molecule magnets *Nature* **468** 417-421

Manoli M, Johnstone R D L, Parsons S, Murrie M, Affronte M, Evangelisti M and Brechin E K (2007) A Ferromagnetic Mixed-Valent Mn Supertetrahedron: Towards Low-Temperature Magnetic Refrigeration with Molecular Clusters *Angew Chem Int Ed* **46** 4456-4460

Milios C J, Vinslava A, Wood P A, Parsons S, Wernsdorfer W, Christou G, Perlepes S P and Brechin E K (2006) A Single-Molecule Magnet with a "Twist" *J Am Chem Soc* **129** 8

Milios C J, Vinslava A, Wernsdorfer W, Moggach S, Parsons S, Perlepes S P, Christou G and Brechin E K (2007) A Record Anisotropy Barrier for a Single-Molecule Magnet *J Am Chem Soc* **129** 2754-2755

Morrish A H (1966) The Physical Principles of Magnetism. Wiley, New York

Mukherjee A, Raghunathan R, Saha M K, Nethaji M, Ramasesha S and Chakravarty A R (2005) Magnetostructural Studies

on Ferromagnetically Coupled Copper(II) Cubanes of Schiff-Base Ligands *Chem Eur J* **11** 3087-3096

Mukherjee S, Chaudhari A K, Xue S, Tang J and Ghosh S K (2013) An asymmetrically connected hexanuclear Dy^{III}_6 cluster exhibiting slow magnetic relaxation *Inorg Chem Commun* **35** 144-148

Mukherjee S, Joarder B, Xue S, Tang J and Ghosh S K (2014) Slow Magnetic Relaxation in an Asymmetrically Coupled Heptanuclear Dysprosium(III)–Nickel(II) Architecture *Proc Natl Acad Sci India, Sect A Phys Sci* **84** 151-156

Murugesu M (2012) Magnetic anisotropy: The orientation is in the details *Nat Chem* **4** 347-348

Nayak S, Evangelisti M, Powell A K and Reedijk J (2010) Magnetothermal Studies of a Series of Coordination Clusters Built from Ferromagnetically Coupled $\{Mn^{II}_4Mn^{III}_6\}$ Supertetrahedral Units *Chem Eur J* **16** 12865-12872

Palacios M A, Titos-Padilla S, Ruiz J, Herrera J M and Pope S J A (2014) Bifunctional $Zn^{II}Ln^{III}$ Dinuclear Complexes Combining Field Induced SMM Behavior and Luminescence: Enhanced NIR Lanthanide Emission by 9-Anthracene Carboxylate Bridging Ligands *Inorg Chem* **53** 1465-1474

Palomo C, Oiarbide M and García J.M. (2002) The Aldol Addition Reaction: An Old Transformation at Constant Rebirth *Chem Eur J* **8** 36

Randell N M, Anwar M U, Drover M W, Dawe L N and Thompson L K (2013) Self-Assembled $Ln(III)_4$ (Ln = Eu, Gd, Dy, Ho, Yb) [2×2] Square Grids: a New Class of Lanthanide Cluster *Inorg Chem* **52** 6731-6742

Rinehart J D, Fang M, Evans W J and Long J R (2011) Strong exchange and magnetic blocking in N_2^{3-}-radical-bridged lanthanide complexes *Nat Chem* **3** 538-542

Rinehart J D and Long J R (2011) Exploiting single-ion anisotropy in the design of f-element single-molecule magnets *Chem Sci* **2** 2078-2085

Sessoli R, Hui L, Schake A R, Wang S, Vincent J B, Folting K, Gatteschi D and Christou G (1993) High-Spin Molecules: $[Mn_{12}O_{12}(O_2CR)_{16}(H_2O)]$ *J Am Chem Soc* **115** 1804-1816

Sessoli R, Gatteschi D, Caneschi A and Novak M A (1993) Magnetic bistability in a metal-ion cluster *Nature* **365** 141-143

Stamatatos T C, Albiol D F, Wernsdorfer W, Abbouda K A and Christou G (2011) High-nuclearity, mixed-valence Mn_{17}, Mn_{18} and $\{Mn_{62}\}_n$ complexes from the use of triethanolamine *Chem Commun* **47** 274-276

Tang J K, Hewitt I, Madhu N T, Chastanet G, Wernsdorfer W, Anson C E, Benelli C, Sessoli R and Powell A K (2006) Dysprosium Triangles Showing Single-Molecule Magnet Behavior of Thermally Excited Spin States *Angew Chem Int Ed* **45** 1729-1733

Tian H, Guo Y -N, Zhao L, Tang J and Liu Z (2011) Hexanuclear Dysprosium(III) Compound Incorporating Vertex- and Edge-Sharing Dy_3 Triangles Exhibiting Single-Molecule-Magnet Behavior *Inorg Chem* **50** 8688-8690

Tian H, Wang M, Zhao L, Guo Y N, Guo Y, Tang J and Liu Z (2012) A Discrete Dysprosium Trigonal Prism Showing Single-Molecule Magnet Behaviour *Chem Eur J* **18** 442-445

Ungur L, Langley S K, Hooper T N, Moubaraki B, Brechin E K, Murray K S and Chibotaru L F (2012) Net Toroidal Magnetic Moment in the Ground State of a $\{Dy_6\}$. Triethanolamine Ring *J Am Chem Soc* **134** 18554-18557

Urdampilleta M, Nguyen N V, Cleuziou J P, Klyatskaya S, Ruben M and Wernsdorfer W (2011) Molecular Quantum Spintronics: Supramolecular Spin Valves Based on Single-Molecule Magnets and Carbon Nanotubes *Int J Mol Sci* **12** 6656-6667

Watanabe A, Yamashita A, Nakano M, Yamamura T and Kajiwara T (2011) Multi-Path Magnetic Relaxation of Mono-Dysprosium (III) Single-Molecule Magnet with Extremely High Barrier *Chem Eur J* **17** 7428-7432

Woodruff D N, Winpenny R E P and Layfield R A (2013) Lanthanide Single-Molecule Magnets *Chem Rev* **113** 5110-5148

Wybourne, B G (1965) Spectroscopic Properties of Rare Earths. John Wiley and Sons, New York

Xu G F, Wang Q L, Gamez P, Ma Y, Cleràc R, Tang J, Yan S P, Cheng P and Liao D Z (2010) A promising new route towards single-molecule magnets based on the oxalate ligand *Chem Commun* **46** 1506-1508

Xue S, Zhao L, Guo Y N, Zhang P and Tang J (2012) The use of a versatile o-vanilloyl hydrazone ligand to prepare SMM-like Dy_3 molecular cluster pair *Chem Commun* **48** 8946-8948

Yang C I, Yang S F, Hung S P, Lee G H, Wurd C S and Tsai H L (2011) Mixed-metal single-molecule magnets: Syntheses, structure, and magnetic properties of $[Mn_8Fe_4O_{12}(O_2CR)_{16}(H_2O)_4]$ (R = CH_2Cl, CH_2Br, $CHCl_2$) *Polyhedron* **30** 2969-2977

Yoshihara D, Karasawa S and Koga N (**2008**) Cyclic Single-Molecule Magnet in Heterospin System *J Am Chem Soc*

130 10460-10461

Y Z Tong, Wang Q L, Yang G, Yang G M, Yan S P, Liao D Z and Cheng P (2010) Hydrolytic synthesis and structural characterization of five hexanuclear oxo-hydroxo lanthanide clusters *Cryst Eng Comm* **12** 543-548

Zaleski C M, Depperman E C, Kampf J W, Kirk M L and Pecoraro V L (2004) Synthesis, Structure, and Magnetic Properties of a Large Lanthanide-Transition-Metal Single-Molecule Magnet *Angew Chem Int Ed* **43** 3912-3914

Zhang P, Guo Y N and Tang J (2013) Recent advances in dysprosium-based single molecule magnets: Structural overview and synthetic strategies *Coord Chem Rev* **257** 1728-1763

Zheng Y Z, Lan Y, Anson C E and Powell A K (2009) Anion-Perturbed Magnetic Slow Relaxation in Planar {Dy4} Clusters *Inorg Chem* **47** 10813-10815

Zheng Y Z, Xue W, Zhang W X, Tong M L and Chen X M (2007) From Pseudo to True C_3 Symmetry: Magnetic Anisotropy Enhanced by Site-Specific Ligand Substitution in Two Mn_{15}-Carboxylate Clusters *Inorg Chem* **46** 6437-6443.